九州大学学術情報リポジトリ
Kyushu University Institutional Repository

Phosphatidylserine Containing Liposomes Suppress Inflammatory Bone Loss in the Ankle Joints of Adjuvant Arthritic Rats

馬, 紅梅
九州大学大学院歯学研究院口腔常態制御学講座

https://doi.org/10.15017/19944

出版情報：九州大学, 2010, 博士（歯学）, 課程博士
バージョン：
権利関係：

KYUSHU UNIVERSITY

Phosphatidylserine Containing Liposomes Suppress Inflammatory Bone Loss in the Ankle Joints of Adjuvant Arthritic Rats

2010

Ma Hongmei

Department of Aging Science and Pharmacology,

Faculty of Dental Sciences, Kyushu University

Supervisor:

Professor Nakanishi Hiroshi

A part of the present thesis has been reported in the following paper.

1. Wu Z, Ma HM, Kukita T, Nakanishi Y, Nakanishi H.

Phosphatidylserine-containing liposomes inhibit the differentiation of osteoclasts and trabecular bone loss.

J Immunol. 2010 Mar 15;184(6):3191-201. Epub 2010 Feb 22.

2. Ma Hongmei Wu Zhou, and Nakanishi Hiroshi

Phosphatidylserine-Containing Liposomes Suppress Inflammatory Bone Loss by Ameliorating the Cytokine Imbalance in the Ankle Joints of Adjuvant Arthritic Rats. Lab Invest.(2010) in press.

A part of the present thesis has been reported in the following academic conferences.

1. Wu Z, Ma HM, Kukita T, Nakanishi Y, Nakanishi H.

Phosphatidylserine-liposomes suppress the bone destruction by regulating the cytokine balance and osteoclastogenesis.

The Joint Meeting of the 3rd Symposium on "Oral Health Science" and the 3rd Symposium on "Dental and Craniofacial Morphogenesis and Tissue Regeneration". 26th. Jan. 2008 Fukuoka

2. 馬　紅梅、武　洲、中西　博

ホスファチジルセリンを含むリポソームはアジュバント関節炎に伴うサイトカインの異常発現を制御する

第　50 回歯科基礎医学会学術大会ならびに総会　　2008 年　9 月 23 －　25 日　東京

3. Hongmei Ma , Zhou Wu, Toshio Kukita, Katsumasa Maeda and Hiroshi Nakanishi

Phosphatidylserine-containing liposomes suppress inflammatory bone destruction by phenotypic switching of macrophages and T cells

The International Joint Symposium on “Dental and Craniofacial Morphogenesis and Tissue Regeneration”and“Oral Health Science”. 4th. Feb.2009 Fukuoka

4．武　洲、馬　紅梅、久木田　敏夫、中西　博

ホスファチジルセリン（ ps ）リポソームによる炎症性骨破壊抑制メカニズムの解析

第　52 回歯科基礎医学会学術大会ならびに総会　　2010 年　9 月 20 －　22 日　東京

5．馬　紅梅、武　洲、李　銀姫、久木田　敏夫、中西　博

ホスファチジルセリン（ ps ）リポソームによる骨形成の促進

第　52 回歯科基礎医学会学術大会ならびに総会 2010 年　9 月　20 －　22 日　東京

6. Hongmei Ma , Zhou Wu, Toshio Kukita, and Hiroshi Nakanishi

Phosphatidylserine-Containing Liposomes Suppress Inflammatory Bone Loss by Ameliorating the Cytokine Imbalance in the Ankle Joints of Adjuvant Arthritic Rats

1st Asia-Pacific osteoporosis Meeting 10th ～　13th. Dec. 2010 Singapore

Abbreviations used

PS: phosphatidylserine

PC: phosphatidylcholine

NBD: 4-nitrobenz-2-oxa-1, 3-diazole

TGF β1: transforming growth factor β1

PG E_2: prostaglandin E_2

RANK: receptor activator of NF-κB

RANKL: receptor activator of NF-κB ligand

ICAM-1: intercellular adhesion molecule-1

AA: adjuvant arthritis

IL-1β: interleukin 1β

LPS: lipopolysaccharide

MAPKs: mitogen-activated protein kinases

ERK: extracellular signal-regulated kinase

RA: rheumatoid arthritis

OP: osteoclast precursor

α-MEM: α -Minimum essential medium

$1\alpha,25(OH)_2D_3$: 1α, 25-dihydroxy vitamin D_3

FBS: fetal bovine serum

MNCs: multinucleated cells

CTR: calcitonin receptor

BM: bone marrow

htROSCM: ROS17/2.8 cell-conditioned medium

TRAP: tartrate-resistant acid phosphatase

μCT: microcomputed tomographic

3D: three dimensions

CFA: complete Freund’s adjuvant

DMEM: Dulbecco’s Modified Eagle's Medium

BV/TV: trabecular bone volume per unit of metaphysic

PB: peripheral blood

H-E: Hematoxylin-Eosin

Contents

Abstract

Liposomes containing phosphatidylserine (PS) are engulfed by phagocytes including macrophages, microglia and dendritic cells. PS liposomes mimic the effects of apoptotic cells on these phagocytes to induce the secretion of anti-inflammatory molecules and to inhibit the maturation of dendritic cells. Thus, the interplay between PS liposomes and phagocytes seem to create a microenvironment that can suppress immune and inflammatory responses. However, the effects of PS liposomes on osteoclasts, which are also differentiated from the common myeloid precursors, and the inflammatory bone loss are unknown.

In chapter I of the present study， the direct effects of PS liposomes on the osteoclastogenesis were investigated. In the rat bone marrow culture system, osteoclast precursors phagocytozed PS liposomes to secrete transforming growth factor (TGF) β1 and prostaglandin (PG) E_2, which in turn inhibited osteoclastogenesis through the down-regulation of receptor activator for NF-κB ligand (RANKL), receptor activator of NF-κB (RANK), intercellular adhesion molecule-1 (ICAM-1) and CD44. In consistence with these in vitro observations, intramuscular injection of PS liposomes significantly increased the plasma level of TGF-β1 and PGE_2 and decreased the expression of RANKL, RANK and ICAM-1 in the skeletal tissues of ankle joints of adjuvant arthritis (AA) rats. A quantitative analysis using micro computed tomography revealed that PS liposomes as well as TGF-β1 together with PGE_2 significantly inhibited AA-induced trabecular bone loss.

In chapter II of the present study, the effects of PS liposomes on the phenotypic change of infiltrated macrophages, which were considered indirectly inhibiting osteoclastogenesis during inflammatory bone loss, were elucidated. In the ankle joints of AA rats, approximately half of the infiltrated macrophages

underwent a phenotypic change from interleukin (IL)-1β-producing to IL-10-producing cells after the phagocytosis of PS liposomes. In lipopolysaccharide (LPS)-stimulated macrophages, PS liposomes significantly decreased the IL-1β production, but increased the IL-10 production. Moreover, PS liposomes inhibited the rapid activation of p38 mitogen-activated protein kinases (MAPK) and NF-κB, but enhanced the delayed activation of extracellular signal-regulated kinase (ERK) in LPS-stimulated macrophages. The differential of PSL-induced influences on the activities of p38 MAPK and ERK is a likely underlying mechanism for phenotypic change of infiltrated macrophages after the phagocytosis of PS liposomes. This phenotypic change may be responsible for a significant decrease in the mean mRNA level of RANK and RANKL in the ankle joint of PS liposome-treated AA rats, resulting in the inhibition of inflammatory bone loss.

In conclusions, these observations strongly suggest that phagocytosis of PS liposomes can strongly inhibit AA-induced bone loss through both the direct inhibitory effects on osteoclastogenesis and the indirect effects on changing the infiltrated macrophages from pro-inflammatory to anti-inflammatory phenotype. Therefore , PS liposomes may be potentially useful for achieving pharmacological intervention against inflammatory bone loss in many diseases such as rheumatoid arthritis (RA) and periodontitis without any apparent deleterious side effects.

Chapter I
Phosphatidylserine-Containing Liposomes Inhibit the Differentiation of Osteoclasts and Trabecular Bone Loss

Introduction

Phagocytic cells in the living body play special roles depending on their location and physiological state. Mononuclear cells, including monocytes in the blood, macrophages in the spleen, microglia in the brain and Kupffer cells in the liver, phagocytoze apoptotic cells and necrotic cell debris in the tissues (1). Besides these professional phagocytes, recent reports have shown that non-professional phagocytes such as dendritic cells, the most professional antigen presenting cells, can phagocytoze apoptotic cells (2, 3). Furthermore, osteoclasts, the multinucleated bone cells, which generally remove mineralized matrix resulting in bone resorption, can also phagocytoze apoptotic bone cells (4, 5).

Recognition and removal of apoptotic cells by phagocytes is mediated by changes in plasma membrane on dying cells. One of the most striking and consistent changes on the cell surface of apoptotic cells is the exposure of phosphatidylserine (PS). PS is an anionic aminophospholipid restricted mostly to the inner leaflet of the plasma membrane in live cells (6). However, when cells undergo apoptosis, PS molecules are exposed on the cell surface (7, 8). Exposure of PS plays a central role in the recognition and phagocytosis of apoptotic cells by macrophages (9, 10). There is increasing evidence that PS-dependent phagocytosis of apoptotic cells transform macrophages to an anti-inflammatory phenotype (11-13). On the other hand, phagocytosis of apoptotic cells inhibits the maturation of dendritic cells and their secretion of pro-inflammatory cytokines (2, 14). PS liposomes can mimic the effects of apoptotic cells on macrophages and microglia to induce the secretion of anti-inflammatory

mediators including TGF-β1 and PGE_2 (15, 16). Moreover, PS liposomes inhibit the maturation of dendritic cells and enhance their secretion of anti-inflammatory cytokines (17).

Osteoclasts are differentiated from the common myeloid precursors with macrophages and dendritic cells depending the kinds and amount of factors in the bone marrow microenvironment (18, 19). However, it is not known how PS liposomes affect the osteoclastogenesis. It is well known that receptor activator for NF-κB ligand (RANKL) / receptor activator of NF-κB (RANK) signal plays essential roles in differentiation and the fusion of the precursors into mature osteoclasts (20-23). In addition, the RANKL/RANK pathways are primarily involved in trabecular bone loss in the adjuvant arthritic (AA) rats (24). On the other hand, intercellular adhesion molecule-1 (ICAM-1) and CD44 are known as the important adhesion molecules for the fusion of osteoclast precursor (OP) cells in osteoclastogenesis (25-27). This study attempted to elucidate the effects of PS liposomes on osteoclastogenesis in a rat bone marrow culture systems and the bone loss following the AA, a widely used bone destruction model. The present study highlights the novel role of PS liposomes that inhibit both osteoclastogenesis and AA-induced bone loss through the secretion of TGF-β1 and PGE_2.

Materials and Methods

Reagents

Minimum essential medium α medium (α-MEM) was from GIBCO BRL (Grand Island, NY, USA). 1α, 25-dihydroxyvitamin D_3 ($1\alpha,25(OH)_2D_3$) and SQ22536 were from BIOMOL Research Laboratories Inc. (Plymouth Meeting, PA, USA). Fetal bovine serum (FBS) was from Bio Whittaker (Walkersville, MD, USA). sRANKL was from Peprotec Science (London, England). TGF-β1

was from AbD Serotec (Kidlington Oxford UK) PGE_2 was from Cayman Chemical (Ann Arbor, MI, USA). PS, phosphatidylcholine (PC), 4-nitrobenz-2-oxa-1, 3-diazole (NBD)-labeled PS, and NBD-labeled PC were from Avanti Polar Lipids (Alabaster, AL, USA). Rabbit polyclonal anti-TGF-β1 typeII receptor (TGF-βRII), anti-RANKL, anti-RANK, anti-OPG, mouse monoclonal anti-ICAM-1, anti-CD44, goat polyclonal anti-calcitonin receptor (CTR), normal rabbit IgG were from Santa Cruz Biotechnology Inc. (Santa Cruz, CA USA), monoclonal anti-ED1 was from BMA (Augst, Switzerland), mouse anti-actin was from abcam.com. (Tokyo, Japan). Texas Red-conjugated phalloidin was from Molecular Probes (Eugene, OR, USA). Heat-killed *Mycobacterium butyricum* and mineral oil were from Difco (Detroit, ML, USA).

Liposome

PS liposomes consisted of PC and PS at a molar ratio of 7:3, and PC liposomes consisted of PC only, PS liposomes and PC liposomes were prepared as described previously (16). In some experiments, NBD-labeled PS and PC were used for preparing NBD-labeled PS liposomes and PC liposomes, respectively.

Animals

Female Lewis rats (4-5 weeks old) were from Kyudo co., Ltd. (Fukuoka, Japan) and cared according to the manual of Animal Care and Use Committee, Kyushu University.

Rat cell cultures for forming osteoclasts precursor (OP) cells and osteoclast-like multinucleated cells (MNCs)

Two rat osteoclast-like MNCs generating culture systems, bone marrow (BM) and OP cell cultures, were used in current study as previously described (28, 29). For BM cell culture, whole BM cells were flushed out from tibia and femurs of rats, and cultured in 24-multiwell culture plates (1×10^6 cells/well) in α-MEM with 15 % FBS, 10^{-8} M $1\alpha,25(OH)_2D_3$ and 10 % (v/v) ROS17/2.8 cell-conditioned medium (htROSCM) for 96 h. For OP cell cultures, osteoblasts and stromal cells were depleted from BM cell culture using a Sephadex G10 columm, and then remaining cells were cultured in 24-multiwell culture plates (1×10^6 cells/well) in α-MEM with 15% fetal bovine serum (FBS), 10^{-8} M 1α, $25(OH)_2D_3$, 10 % (v/v) htROSCM for 96 h. In this culture condition, only mononuclear TRAP-positive cells were formed as OP cells (28). OP cells were cultured in 24-multiwell culture plates (1×10^6 cells/well) for 96 h in α-MEM with 15 % fetal bovine serum (FBS), 10^{-8} M $1\alpha,25(OH)_2D_3$, 10 % (v/v) htROSCM and sRANKL (20 ng/ml) for 96 h. Various concentrations of PS liposomes, PC liposomes and chemical components were added to the BM and OP cell cultures. At the day 4 (96 h) of the cultures, cells was fixed by 4 % paraformaldehyde in PBS for 30 min, and staining with tartrate-resistant acid phosphatase (TRAP) kit (Sigma-Aldrich), the general marker of osteoclast. TRAP-positive cells with more than three nuclei were counted as osteoclast-like MNCs (mature osteoclasts).

Western blotting

PS liposomes treated or untreated BM and OP cell extracts were prepared with cell lysis buffer (16) and western blots were performed with the following antibodies: rabbit polyclonal anti-RANKL (1:500 dilution), anti-RANK (1:500 dilution), anti-OPG (1:500 dilution) or anti-actin (1:2000 dilution). Blots were

final detected by enhanced chemiluminescence detection system (ECL kit, Amersham Bioscience, Uppsala, Sweden) and quantified with image analyzer FLA3000 (Fuji Photo Film, Tokyo, Japan). Values were normalized to actin.

Flow cytometry analysis

OP cells were treated with PS liposomes (100 μM), TGF-β1 (500ng/ml) or PGE_2 (500 ng/ml). After removed by cell dissociation buffer enzyme-free PBS-based (GiBCO) at each time point, the cells (5×10^5) were incubated with mouse monoclonal ICAM-1 (1:200) or anti-CD44 (1:200) antibodies for 1h on ice, normal mouse IgG as negative control. After washes by PBS with 2 % FBS, the cells were incubated for 30 min on ice with donkey anti-mouse FITC-labeled IgG. After washes by PBS with 2 % FBS, immunofluorescence was analyzed using a FAC Scan analyzer (Becton Dickinson, San Jose, CA, USA).

Systemic PS liposomes treatment for adjuvant arthritic rats and samples preparing

Female Lewis rats (5-weeks old, n=120) were used in vivo experiments. The animals (n=93) were injected intradermally with CFA (1.5 mg heat-killed Mycobacterium butyricum well suspended in 0.15 ml mineral oil) at the base of the tail to induce adjuvant arthritis (AA) as we described previously (30, 31). Rats were injected with mineral oil only as sham rats (n=27). We injected intramuscularly with PS liposomes (5 mg/kg/day, PS liposomes-treated AA rats n=27) or PC liposomes (5mg/kg/day, PC liposome-treated AA rats, n=27) in the hind limbs from days 14 to 28 after CFA injection. At this time point, acute synovial inflammation of ankle joints was confirmed without bone destruction occurring (31, 32). The AA rats injected intramuscularly with PBS as the AA rats

(n=27). Rats were anesthetized with sodium pentobarbital (30 mg/kg, i.p.) at day 2, 7 and 14 after PS liposomes or PC liposomes treatment. After obtaining the blood samples, animals were perfuse intracardially with 2 % paraformaldehyde fixative in PBS. The ankle joints were removed and immersed in the same fixative for 12 h at 4 ℃. Some samples were for microcomputed tomographic (μCT) analyses (n=6), other samples were decalcified in 10% EDTA for another 3 weeks. After immersing in 30% sucrose in PBS for 2 days, samples were embedded in an optimal cutting temperature compound (Sakura Finetechnical Co., Ltd., Tokyo, Japan). Serial coronal frozen sections (10 μm) were prepared for histoglical and immunohistochemistry as described previously (31). For real-time PCR analyses, the rats (n=3 of each time point) were perfuse intracardially with PBS, the ankle joints were removed and stored at -80℃. In other groups, we injected intramuscularly with TGF-β1 (25 μg/kg/day) and PGE_2 (2.5 μg/kg/day) from days 14 to 28 after CFA injection at same time course of PS liposomes treatment on AA rats (n=6). We also injected intramuscularly with anti-TGF-β1 antibody (100 μg/kg/day) and SQ22536 (125 μg/kg/day) from day 12, and then treatment with PS liposomes from days 14 to 28 after CFA injection (n=6). Rats were anesthetized with sodium pentobarbital (30 mg/kg, i.p.) and perfused intracardially with 2 % paraformaldehyde fixative in PBS after 14 days of the treatments. The ankle joints were removed and immersed in the same fixative for μCT analyses.

μCT analysis

The ankle joints of sham, AA rats and the AA rats at days 14 after the treatments of each group (n=6) were examined using ScanXmate-E090S40 in vivo (Comscantecno, Co. Ltd, Kanazawa, Japan). In briefly, rat paws were scanned, the bones including tibia, talus and calcaneus in the ankle joints were

examined by three dimensions (3D) surface rendering with a common threshold, optimized using histomorphometric techniques (GEMS MicroView). Because the trabecular bone loss within the tibia and talus in the AA rats were too severe to quantify, calcaneuses were used for bones qualitative analysis. The parameters of trabecular bone in each group were analyzed using TRI/3D-BON software (Ratoc System Engineering Co.Ltd. Tokyo, Japan).

ELISA

Plasma samples from rats and the supernatants of cultured cells were measured using TGF-β1 (R&D, Minneapolis, USA) and PGE_2 (Amersham Bioscience, Uppsala, Sweden) ELISA kits. The assay was following the protocol provided by the manufacturer. The absorbency at 450 nm was performed by a microplate reader (Bio-Red Laboratories. Hercules, CA, USA).

Immunohistochemistry

The sections of ankle joints from sham and the AA rats were blocked with 10% normal donkey serum, and were incubated with monoclonal anti-ICAM-1 IgG (1:100) overnight at 4 ℃. After being incubated with biotinylated anti-mouse IgG (1:200, Jackson Immunoresearch Lab. Inc., West Grove, USA) for 2 h at 24 ℃, the sections were incubated with peroxidase-conjugated streptavidin (1:300, Dako Japan, Kyoto, Japan) for 30 min at 24 ℃. The peroxidase was developed using 3,3’-diaminobenzidine (DAB substrate kit, Vector Lab. Inc., Burlingame, CA, USA), Mayer’s hematoxylin was used counterstained.

Immunofluorescence

NBD-labeled PS liposomes (100 μM) or NBD-labeled PC liposomes (100 μM) was applied to cultured OP cells in chamber slides (Nalgen Nunc International. Rochester, NY USA), and the cells were obtained from 24 to 96 h. In the in vivo experiments, after 6 h of systemic treatment with NBD-labeled PS liposomes (5 mg/kg) or NBD-labeled PC liposomes (5 mg/kg) in the AA rats, bone marrow cells and peripheral blood cells were obtained and incubated in chamber slides (2×10^5 cells/well) at 37 ℃ for another 24 h. The cells were fixed with 2 % paraformaldehyde for 30 min at 24 ℃. The cultured cells and the cells from bone marrow and peripheral blood of the AA rats were incubated with mouse anti-ED1 (1:400) or goat anti-CTR (1:200) overnight at 4℃. After wash with PBS, the slides were incubated rhodamine-conjugated donkey anti-mouse or goat IgG for 1h at 24 ℃. In some experiments, culture cells were incubated with Texas Red-conjugated phalloidin for visualizing the margins of OP cells. In the separated experiments, the ankle joint sections were incubated with anti-goat CTR antibody mixed with anti-mouse ICAM-1 overnight at 4 ℃. After being incubated with a mixture of FITC-conjugated donkey anti-mouse IgG and rhodamine-conjugated donkey anti-goat IgG for 1h at 24 ℃, the slides were mounted in anti-fading medium Vecta shield (Vector Laboratory) and examined by a confocal laser scanning microscope LSM510MET (Carl Zeiss, Jena, Germany).

Real-time RT-PCR

Skeletal tissues of ankle joints of rats were obtained after removed the soft tissues. RNA from the skeletal tissues was extracted with RNeasy Lipid Tissue Midi Kit (QIAGEN, Germany) according to the manufacturer's instructions. RNA was reversely transcribed to cDNA using PrimeScript™ RT reagent Kit (Takara, Japan). The real-time RT-PCR was performed using SYBR® Premix Ex

Taq™ (Takara, Japan). The thermal cycling was holding at 95 ℃ for 10 min, followed by 30 cycles of 95 ℃ for 15 s, and 60 ℃ for 30 s. After amplifying PCR reaction, melting curve analysis was performed from 55 ℃ to 95 ℃ (0.5 ℃ /S). GAPDH was used as an internal control. The standard curve method using for quantification of gene expression, target gene/ GAPDH were compared between the AA rats and sham rats, and the PS liposomes or PC liposomes treated AA rats between the untreated AA rats.

Primer sequences were as follows; RANKL: 5'- TCGGGTTCCCATAAAGT CAG -3'and 5'- CTGAAGCAAATGTTGGCGTA -3'; RANK: 5'- ACCTGTCT TCTAAATGCACTC -3' and 5'- CTTGCCTGCATCACAGACTT -3'; OPG: 5'- ACACACCAACTGCAGCTCAC-3' and 5'-TGTCCACCAGAACACTCAGC-3', GAPDH: 5'- AAGTACCCCATTGAACACGG -3' and 5'-ATCACAATGCC AGTGGTACG-3'.

Statistical analysis

Data are expressed as means ± SD. The significant differences between groups were determined with student's *t*-test.

Results

Phagocytosed PS liposomes by osteoclast precursor inhibits rat osteoclastogenesis

The present study used two rat osteoclast generating culture systems: BM and OP cell cultures. BM cell cultures contain the whole BM cells including stromal cells and osteoblasts, while OP cell cultures contain only mononuclear OP cells (29). To assess the effects of PS liposomes on osteoclastogenesis, it was necessary to determine whether PS liposomes could be phagocytosed by OP

cells. To visualize the margin of the cells, OP cells were stained by Texas red-conjugated phalloidin which binds to F-actin. At 24 h after treatment, large granular aggregates of NBD-labeled PS liposomes apparently localized in the cytoplasm of OP cells, which cell marginal F-actin was visualzed by Texas red-conjugated phalloidin (Fig. 1Aa). PS liposomes were also detected in the cytoplasm up to 96 h after treatment (Fig. 1Ad). The merged CLSM images show that NBD-labeled PS liposomes (green) corresponded well with the immunoreactivity for ED1 (red), a lysosomal membrane antigen of rat monocytes (33) (Fig. 1Ab, e), thus suggesting that PS liposomes were transported into the endosome/lysosome of OP cells after engulfment (16). To further elucidate a phagocytosis of PS liposomes by OP cells, CLSM was utilized to construct orthogonal cross sectional images of cultured OP cells that were immunohistochemically stained by an anti-CTR antibody, a marker for OP cells. CLSM images of a plan view with two orthogonal cross sectional views of CTR-labeled cultured OP cells clearly demonstrated that PS liposomes were engulfed by OP cells (Fig. 1Ac, f). However, no granular aggregates of the NBD-labeled PC liposomes were found in OP cells after treatment (Fig. 1Ag, h).

Next, the effects of PS liposomes on the rat osteoclastogenesis were examined using both OP and BM cell cultures. TRAP-positive cells with more than three nuclei are counted as osteoclast-like MNCs. On the other hand, TRAP-positive mononuclear cells, which are considered as OP cells. In the control condition of both BM and OP cell cultures, the TRAP-positive MNCs were not detected until 48 h, and the number of TRAP-positive MNCs peaked at 96 h (Fig. 1B, indicated by red arrows), while some cells still remained as TRAP-positive mononuclear cells (Fig. 1B, blue arrows). Fig. 1B also showed TRAP-negative cells consisting of mainly osteoblasts and stromal cells in BM cell cultures. The effect of PS liposomes on the rat osteoclastogenesis was thus examined in both BM and OP cell cultures at 96 h. PS liposomes significantly

decreased the mean number of TRAP-positive MNCs in a dose-dependent manner in both cell cultures at 96 h (Fig. 1B, C). These results suggest that the primary target of PS liposomes is OP cells to inhibit osteoclastogenesis. As previously noted, the minimal concentration of PS liposomes for a significant inhibition of TRAP-positive MNCs formation in OP cell cultures was lower than that in BM cell cultures. However, PC liposomes did not affect the mean number of TRAP-positive MNCs in either cultured cells at 96 h (Fig. 1C). Next, the stage when PS liposomes inhibited TRAP-positive MNCs formation was determined. As shown in Fig. 1D, the number of TRAP-positive MNCs significantly decreased when application of PS liposomes (100 μM) were started at early stage (from 0 to 48 h) but not at the later stage (from 72 h) in both culture cells. However, PS liposomes did not inhibit the mean number of TRAP-positive mononuclear cells (OP cells) at 96 h (Fig. 1E). These observations strongly suggest that PS liposomes inhibit rat osteoclastogenesis from the precursors by acting on OP cells directly without affecting the precursor formation.

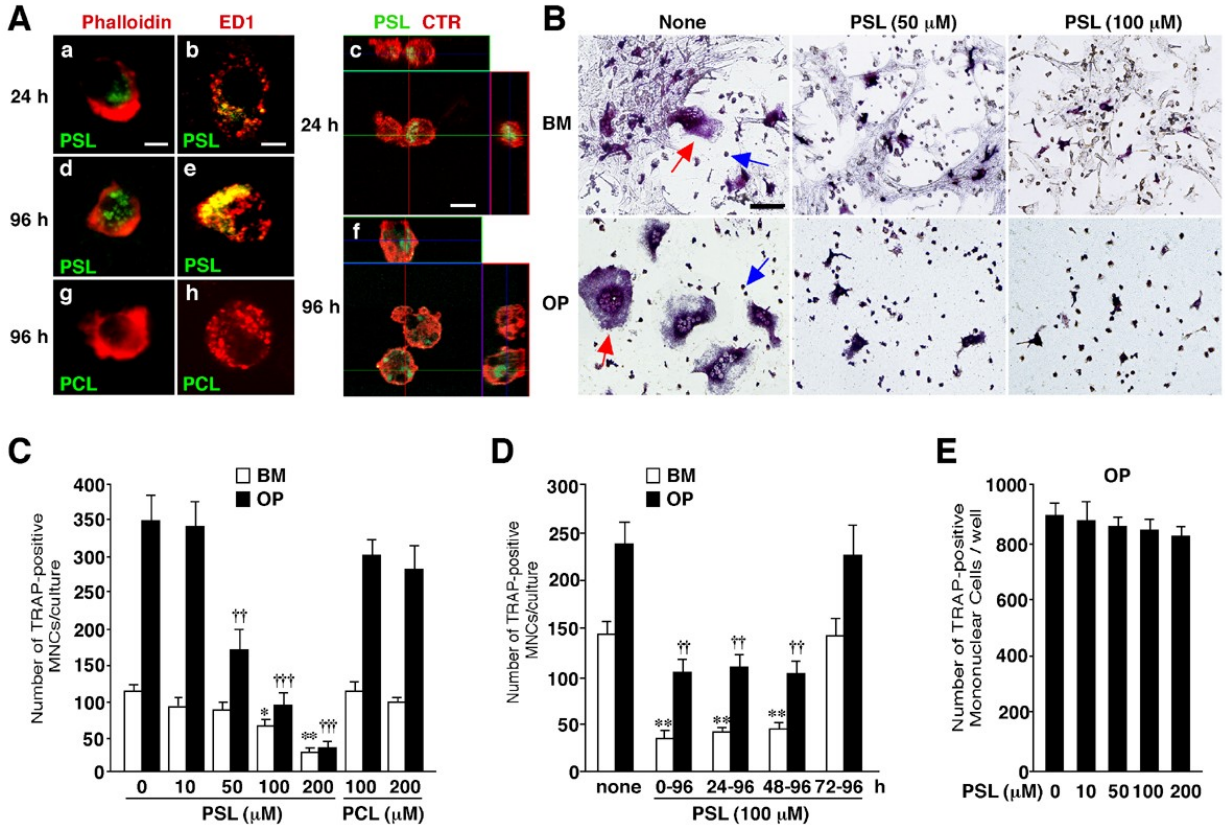

Figure 1 Inhibitory effect of PS liposomes (PSL) on the formation of TRAP-positive multinuclear cells in BM and OP cell cultures.

A, NBD-leveled PSL (green) was phagocytozed by OP cells, stained with phalloidin (red) at 24 h (*a*) and 96 h (*d*) after treatment in cultured OP cells. NBD-leveled PSL co-localized with immunoreactivity for ED1 (red) at 24 h (*b*) and 96 h (*e*) after treatment in cultured OP cells. CLSM images of plan view with two orthogonal cross sectional views clearly showed that PS liposomes were engulfed by OP cells which labeled with anti-CTR antibody at 24 h (*c*) and 96 h (*f*) after treatment. No phagocytosis of NBD-leveled PC liposome (PCL) by OP cells stained by phalloidin (*g*) or anti-ED1 antibody (*h*) was observed even at 96h after treatment (Scale bar, 10 μm in *a*, *b* and 2 μm in *c*). *B*, *C*, The dose dependency of the inhibitory effect of PSL on the rat osteoclastogenesis in BM and OP cell cultures at 96 h. TRAP-positive MNCs and mononuclear cells were

indicated by red and blue arrows, respectively, Scale bar, 50 μm (*B*). PSL significantly inhibited the formation of TRAP-positive MNCs in a dose-dependent manner in both BM and OP cell cultures, PCL did not affect the formation of TRAP-positive MNCs (*C*). *D*, The time dependency effect of PSL on the osteoclastogenesis at 96 h. It was noted that a PSL (100 μM) significantly inhibited osteoclastogenesis in both rat culture cells when applied at an early stage (from 24 to 48 h) but not at the later stage (from 72 h). Each column and bar represents the mean±SD of 3 experiments. The asterisks indicate significant differences between the PSL treated and untreated BM cell cultures (**P*<0.05, ***P*<0.01, Student's *t*-test). The swords indicate significant differences between the PSL treated and untreated OP cell cultures (††*P*<0.01, †††*P*<0.001, Student's *t*-test). *E*, PSL failed to inhibit the formation of TRAP-positive mononuclear OP cells at 96 h. Each column and bar represents the mean±SD of 3 experiments.

PS liposomes down-regulated the expression of RANKL, RANK, ICAM-1 and CD44 in cultured cells

To elucidate the mechanism underlying the inhibitory effects of PS liposomes on the rat osteoclastogenesis, the effects of PS liposomes on the expression levels of RANKL, RANK and OPG, which play essential roles in osteoclastogenesis were examined. The expression of RANKL and OPG was examined in BM cell cultures, because the treatment of sRANKL (20 ng/ml) is required for TRAP-positive MNCs formation in OP cell cultures. The protein amount of RANKL in BM cells increased from 48 h to 72 h during the 96 h-culture period. PS liposomes significantly decreased the mean level of RANKL from 48 h to 72 h (Fig. 2A, B), but not that of OPG (Fig. 2A, C). On the other hand, the protein amount of RANK in OP cell cultures increased from 48h during the culture period. PS liposomes significantly decreased the mean level of RANK from 48 h in OP cell cultures (Fig. 2A, D). Furthermore, PGE_2 significantly decreased the mean level of RANKL in BM cell cultures, but did not affect that of either OPG in BM cell cultures or RANK in OP cell cultures. In contrast, TGF-β1 significantly decreased the mean level of RANK in OP cells from 48 h to 72 h, but did not affect that of either RANKL or OPG in BM cells (Fig. 2A-D). On the other hand, PC liposomes did not affect the mean level of RANKL and OPG in BM cell cultures and that of RANK in OP cell cultures (Fig. 2A-D). Next, the effects of PS liposomes, PC liposomes, TGF-β1 and PGE_2 on the expression of both ICAM-1 and CD44 by cultured OP cells were further examined using flow cytometer, because ICAM-1 and CD44 are involved in the fusion of the precursors into mature osteoclasts (25-27). As shown in Fig. 3A and C, ICAM-1 was expressed in OP cells during the culture period. PS liposomes significantly decreased the number of ICAM-1-positive OP cell cultures to 53.4 % and 75.8 % of the control level at 48 h and 72 h, respectively. In addition, both

TGF-β1and PGE_2 also significantly decreased the number of ICAM-1-positive cells to 77.3 % and 78.2 % of the control level at 48 h respectively. As shown in Fig. 3B and D, CD44 was also expressed in OP cell cultures during the culture times. PS liposomes significantly decreased the number of CD44-positive OP cells to 79.5 % of the control level at 48 h. Furthermore, TGF-β1 but not PGE_2 significantly decreased the number of CD44-positive cells to 86.2 % of the control level at 48 h. It was also noted that PS liposomes, TGF-β1 and PGE_2 did not affect the expression level of either ICAM-1 or CD44 in OP cell cultures at 72 h after treatment. On the other hand, PC liposomes did not affect the expression of both ICAM-1and CD44 in OP cell cultures (Fig. 2C, D). These observations strongly suggest that PS liposomes, TGF-β1 and PGE_2 decreased the expression levels of RANKL, RANK, ICAM-1, and CD44 that are involved in the differentiation and fusion of OP cells.

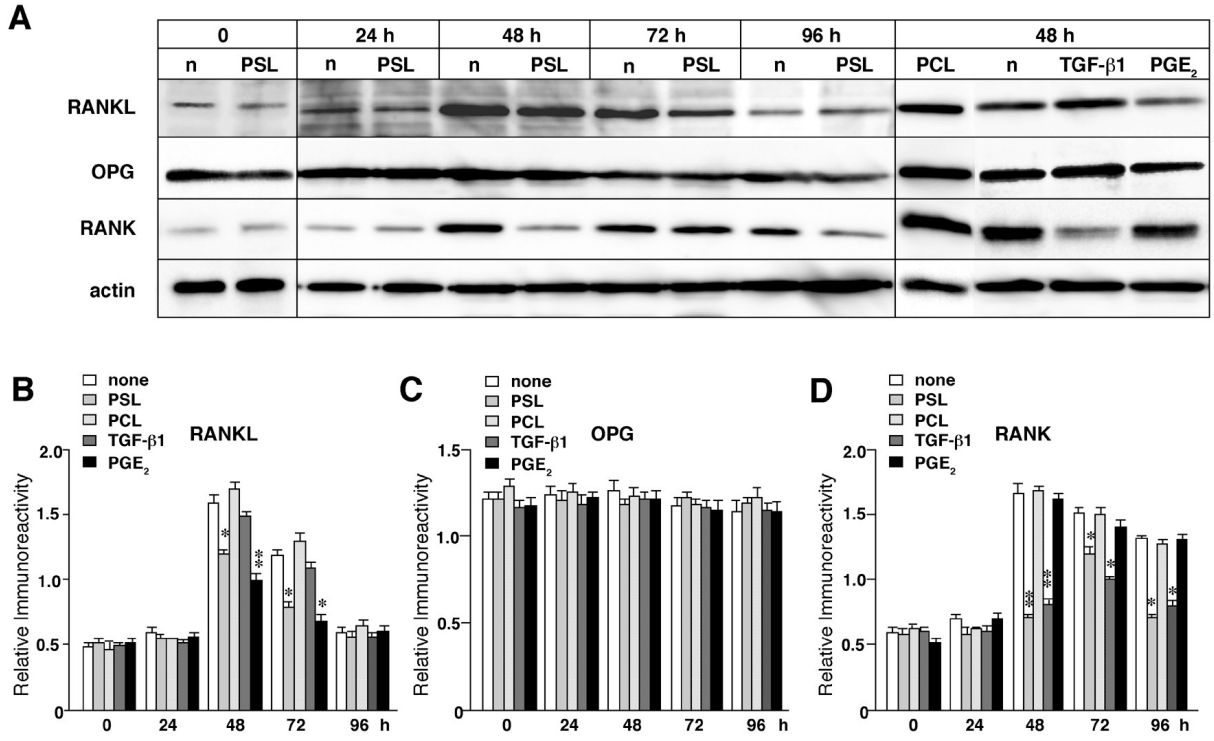

Figure 2 Effects of PS liposomes (PSL), TGF-β1 and PGE_2 on the protein expression of RANKL, RANK and OPG in the rat culture cells.

A, Immunoblot analyses of RANKL, OPG and RANK after treatment with PSL, PC liposomes (PCL), TGF-β1 and PGE_2. *B-D*, The time course changes of RANKL and OPG in BM cell cultures, and RANK in OP cell cultures. The mean protein levels of RANKL (*B*), OPG (*C*) and RANK (*D*) after treatment with PSL, PCL, TGF-β1 and PGE_2. The mean relative immunoreactivity for RANKL, OPG and RANK in untreated and PSL-treated BM or OP cell cultures were determined by comparison to that for actin. Each column and bar represents the mean±SD of 3 experiments. The asterisks indicate significant differences between the PSL-, TGF-β1- and PGE_2-treated and untreated BM or OP cell cultures at each time points (**P*<0.05, ***P*<0.01, Student's *t*-test).

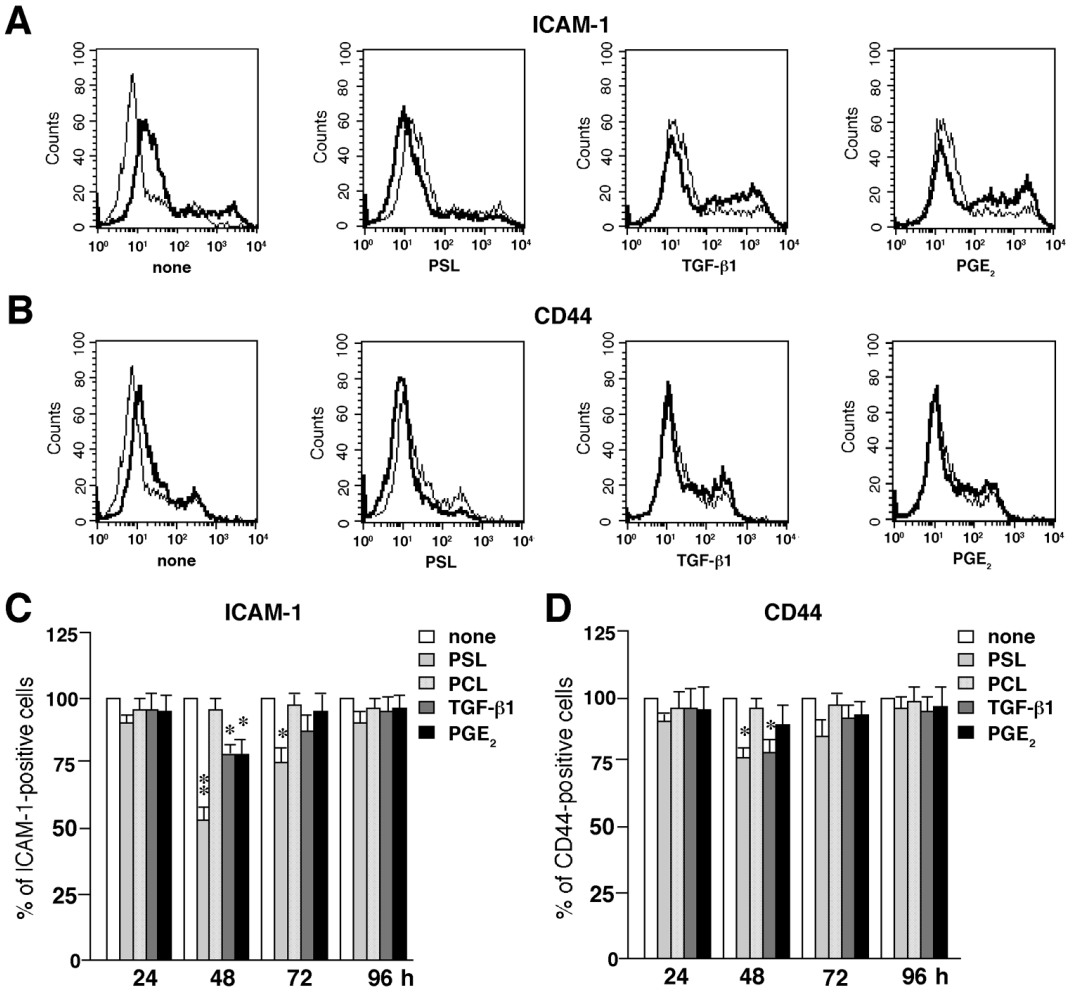

Figure 3 Effects of PS liposomes (PSL), TGF-β1 and PGE_2 on the expression of ICAM-1 and CD44 in OP cell cultures.

A, *B*, Effects of PSL, TGF-β1 and PGE_2 on the expression of ICAM-1 (*A*) and CD44 (*B*) in OP cells at 48 h after treatment. In untreated OP cell cultures, the thick lines represent the ICAM-1- or CD44- expression, and the thin lines represent the controls using mouse IgG, respectively. In treated OP cell cultures, thin lines represent untreated cells and thick lines represent treated with PSL, PGE_2 or TGF-β1, respectively. *C, D,* The time course changes in the mean normalized percentage of ICAM-1-positive cells (*C*) and CD44-positive (*D*) OP cells after treatment with PSL, PC liposomes (PCL), TGF-β1 and PGE_2. Each column and bar represents the mean±SD of 3 experiments. The asterisks indicate

significant differences between the PSL-, TGF-β1- or PGE_2-treated and untreated OP cell cultures (*P<0.05, **P<0.01, Student's t-test).

PS liposomes increases the release of TGF-β1 and PGE_2 and thereby inhibits rat osteoclastogenesis

Next, the effects of PS liposomes on secretion of TGF-β1 and PGE_2 from both BM and OP cells were examined, because PS liposomes can induce the production of these molecules after phagocytozed by macrophages and microglia (11, 16). TGF-β1 release in both culture cells significantly increased from 24 h after PS liposomes treatment in comparison to that in the untreated cells (Fig. 4A), and the increased level of TGF-β1 lasted up to 96 h (data not shown). The release of PGE_2 reached the maximal level at 24 h after treatment with PS liposomes, lasted up to 48 h, the early periods of the culture, and then returned rapidly to the control level thereafter (Fig. 4B). However, no increase of TGF-β1 and PGE_2 was found in either BM or OP cell culture after treatment with PC liposomes (Fig. 4A,B). These observations indicate that OP cells induce the secretion of both TGF-β1 and PGE_2 following phagocytosis of PS liposomes. The roles of TGF-β1 and PGE_2 in osteoclastogenesis are still matters of controversy, depending on the cell types, species and concentrations of these molecules. It has been reported that TGF-β1 enhances osteoclastogenesis even at low concentrations (less than 100 pg/ml), while inhibits it at a higher dose (e.g. 2 ng/ml) (34, 35). Although PGE_2 is generally believed to stimulate osteoclastogenesis in murine cultured cells at a relatively high concentration (36-38), PGE_2 also been shown to inhibit osteoclastogenesis in human and rat culture systems (39-42). Therefore, the effects of TGF-β1 and PGE_2 on rat osteoclastogenesis were examined. As shown in Fig. 4C, TGF-β1 significantly decreased the mean number of TRAP-positive MNCs at the concentration of 500 pg/ml but not 50 pg/ml. The inhibitory effect of TGF-β1 (500 pg/ml) was completely reversed by rabbit anti-TGF-β1RII antibody (5μg/ml), but not control rabbit IgG (Fig. 4C). Furthermore, PGE_2 also significantly inhibited the

formation of TRAP-positive MNCs at the concentration of 500 but not 50 pg/ml. The inhibitory effect of PGE_2 was completely antagonized by SQ22536 (10 μM), a specific inhibitor of adenylate cyclase. It is noted that combined treatment with TGF-β1 (50 pg/ml) and PGE_2 (50 pg/ml) significantly inhibited the formation of TRAP-positive MNCs. Moreover, the inhibitory effect of PS liposomes (100 μM) on the formation of mature osteoclasts was reversed by either rabbit anti-TGF-β1 antibody (5 μg/ml) or SQ22536 (Fig. 4D). However, control rabbit IgG did not affect the inhibitory effects of PS liposomes on the formation of TRAP-positive MNCs (Fig. 4D). PS liposome-induced secretion of either TGF-β1 or PGE_2 in the culture medium did not reach the concentration to inhibit the osteoclastgenesis. Therefore, it is reasonable to consider that PS liposome-induced the inhibition of osteoclastogenesis was mediated by presumable synergistic effect of TGF-β1 and PGE_2.

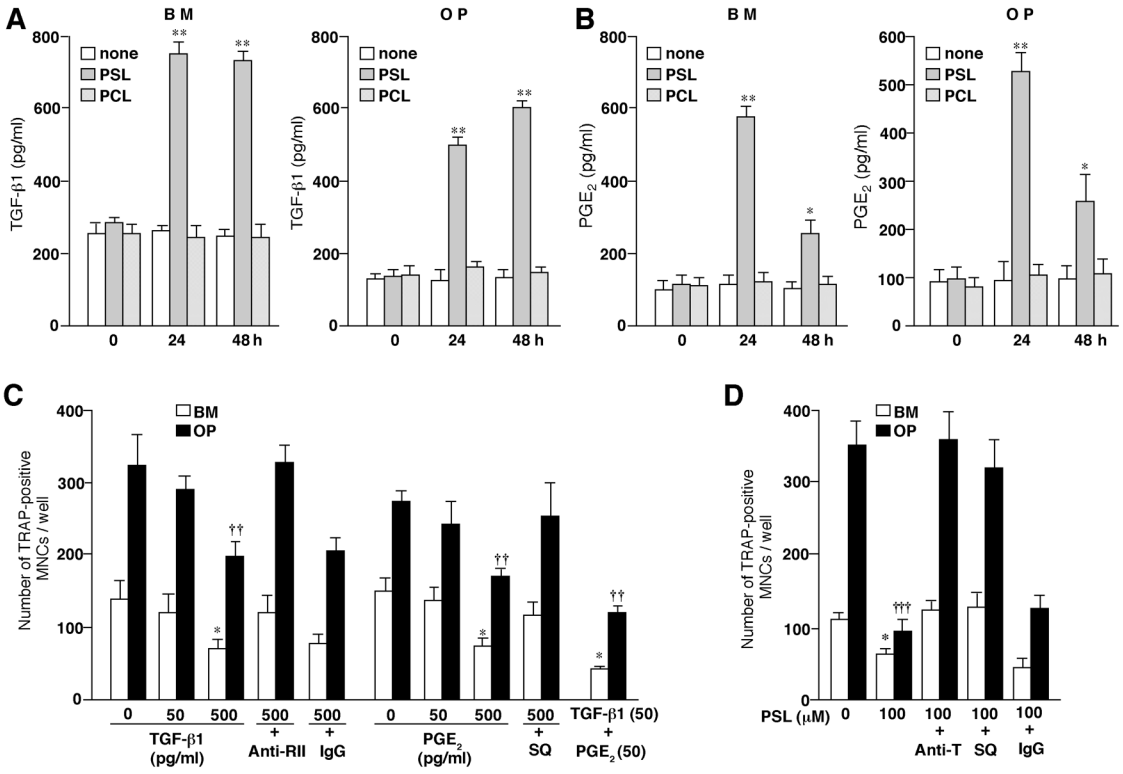

Figure 4 Involvement of TGF-β1 and PGE_2 in PS liposome (PSL)-induced inhibition of osteoclastogenesis in rat BM and OP cell cultures.

A, *B*, Release of TGF-β1 (*A*) and PGE_2 (*B*) from the cultured cells following treatment with PSL and PC liposomes (PCL). Each column and bar represents the mean±SD of 3 experiments. The asterisks indicate significant differences between the PSL treated and untreated BM cell cultures (**P*<0.05, ***P*<0.01, Student's *t*-test). The swords indicate significant differences between the PSL treated and untreated OP cell cultures (†*P*<0.05,††*P*<0.01, Student's *t*-test). *C*, The number of TRAP-positive MNCs was decreased in a dose dependent after treatment with TGF-β1 or PGE_2. TGF-β1- and PGE_2-induced inhibition was reversed by anti-TGF-βRII antibody (Ant-RII) and SQ22536 (SQ), a specific inhibitor for adenylate cyclase, respectively, but was not reversed by control rabbit IgG. The mean number of TRAP-positive MNCs was not affected by either TGF-β1 or PGE_2 alone at the concentration of 50 pg/ml, but was

significantly suppressed by their combined treatment. Each column and bar represents the mean±SD of 3 experiments. An asterisk indicates a significant difference between the PSL treated and untreated BM cells (*P<0.05, Student's t-test). The swords indicate a significant difference between the PSL treated and untreated OP cells (††P<0.01, Student's t-test). *E*, The inhibitory effect of PSL (100 μM) on TRAP-positive MNCs formation was reversed by either anti-TGF-β1 (Anti-T) or SQ22536 (SQ), but was not reversed by control rabbit IgG. Each column and bar represents the mean±SD of 3 experiments. An asterisk indicates a significant difference between the PSL treated and untreated BM cell cultures (*P<0.05, Student's t-test). The swords indicate a significant difference between the PSL treated and untreated OP cell cultures (†††P<0.001, Student's t-test)

Systemic treatment with PS liposomes increases the plasma level of TGF-β1 and PGE_2 and markedly suppresses trabecular bone loss in the AA rats

To confirm the inhibitory effect of PS liposomes on osteoclasts formation *in vivo*, the effects of PS liposomes on an osteoclastic-induced trabecular bone loss model, the AA rats was investigated. Systemic treatment with PS liposomes was initiated 14 days after CFA injection, when the peak of paw inflammation was established. However, the number of osteoclasts increases with bone destruction after the peak of inflammation in the ankle joints of the AA rats (30, 31). At 24 h after intramuscular treatment, CLSM images of a plan view with two orthogonal cross sectional views clearly demonstrated that PS liposomes were engulfed by CTR-labeled OP cells in the tibia marrow (Fig. 5Aa) of the AA rats. In the peripheral blood of the AA rats, CLSM images of a plan view with two orthogonal cross sectional views also clearly demonstrated that PS liposomes localized in ED1-positive lysosomes of mononuclear cells (Fig. 5Ab). The paw volume increase of AA rats occurred in 2 stages, an acute inflammation stage, from days 10 to 21 after CFA injection and the bone/joints destruction stage thereafter (31, 32). As shown in Fig. 5B, systemic treatment with PS liposomes or treatment with TGF-β1 and PGE_2 together significantly reduced the paw volume of AA rats during the bone/joints destruction stages. However, treatment with PC liposomes did not reduce the paw volume of AA rats. Furthermore, treatment with anti-TGF-β1 antibody and SQ22536 together completely reversed the inhibitory effects of PS on the paw volume of AA rats. At day 2 after treatment with PS liposomes, the mean plasma levels of TGF-β1 and PGE_2 in the AA rats significant increased in comparison to those in the PBS- and PC liposomes-treated AA rats, and the significant high plasma level of both TGF-β1 and PGE_2 in the PS liposomes-treated AA rats lasted up to 7 days after PS liposomes treatment (Fig. 5C). The mRNA expression levels of RANKL and

RANK significantly increased in the skeletal tissues of the AA rats from 21 days after CFA injection. Treatment with PS liposomes for 7 days significantly decreased the mean expression levels of both RANKL and RANK in the AA rats, however, treatment with PC liposomes did not decrease the expression level of either RANKL or RANK in the AA rats (Fig. 5D). On the other hand, treatment with PS liposomes for 7 days did not affect the mean expression levels of OPG in the AA rats (Fig. 5D). Furthermore, the number of ICAM-1-positive mononuclear cells, which were identified as CTR-positive OP cells, increased in the bone marrow cavities of the AA rats from 21 days after CFA injection. Treatment with PS liposomes for 7 days markedly decreased the number of ICAM-1-positive OP cells in the AA rats (Fig. 5E). These observations obtained in the AA rats were closely consistent with those obtained in the cultured cells. Therefore, a possible decrease in osteoclast formation decrease was examined in the tibia bone marrow cavity of the AA rats. Consistent with previous observations (32), the number of TRAP-positive MNCs in the bone marrow cavity of the distal epiphysis of tibia rapidly increased from 21 days, and numerous TRAP-positive MNCs were found at 28 days after CFA injection. Systemic treatment with PS liposomes significantly decreased the mean number of TRAP-positive MNCs in the tibia bone marrow cavity of the AA rats, however PC liposomes did not decrease the mean number of TRAP-positive MNCs (Fig. 5F).

To further proof the essential roles of TGF-β1 and PGE_2 in PSL-induced inhibitory effects on the trabecular bone loss in AA rats, we finally quantified the trabecular bone network of the bones in the ankle joints at 14 days after treatments with of PS liposomes or TGF-β1 and PGE_2 together on AA rats (28 days after CFA injection) using μCT analysis. The μCT analysis was conducted in the calcaneus, because trabecular bone losses within the tibia and talus in the AA rats were too severe to quantify. In comparison to the sham rats

(Fig. 6A), a severe trabecular bone loss was observed in the AA rats (Fig. 6B). The AA-induced trabecular bone loss was markedly inhibited by treatment with PS liposomes (Fig. 6C) as well as treatment with TGF-β1 and PGE_2 together (Fig. 6D). However, the AA-induced trabecular bone loss was not inhibited by treatment with PC liposomes (Fig. 6E). Furthermore, the AA-induced trabecular bone loss was not inhibited by treatment with PS liposomes and simultaneous treatment with anti-TGF-β1 antibody and SQ22536 (Fig. 6F). In analysis of the parameters of trabecular bone shown in Fig. 6G-I, PS liposomes as well as TGF-β1 and PGE_2 together significantly inhibited the AA-induced decrease of trabecular bone volume per unit of metaphysis (BV/TV, G), trabecular thickness (Tb/Th, H) and trabecular numbers (Tb/N, I). On the other hand, PC liposomes showed no effect on any parameters in AA-induced trabecular bone loss. Moreover, TGF-β1 antibody and SQ22536 significantly blocked the inhibitory effects of PS liposomes on the AA-induced trabecular bone loss.

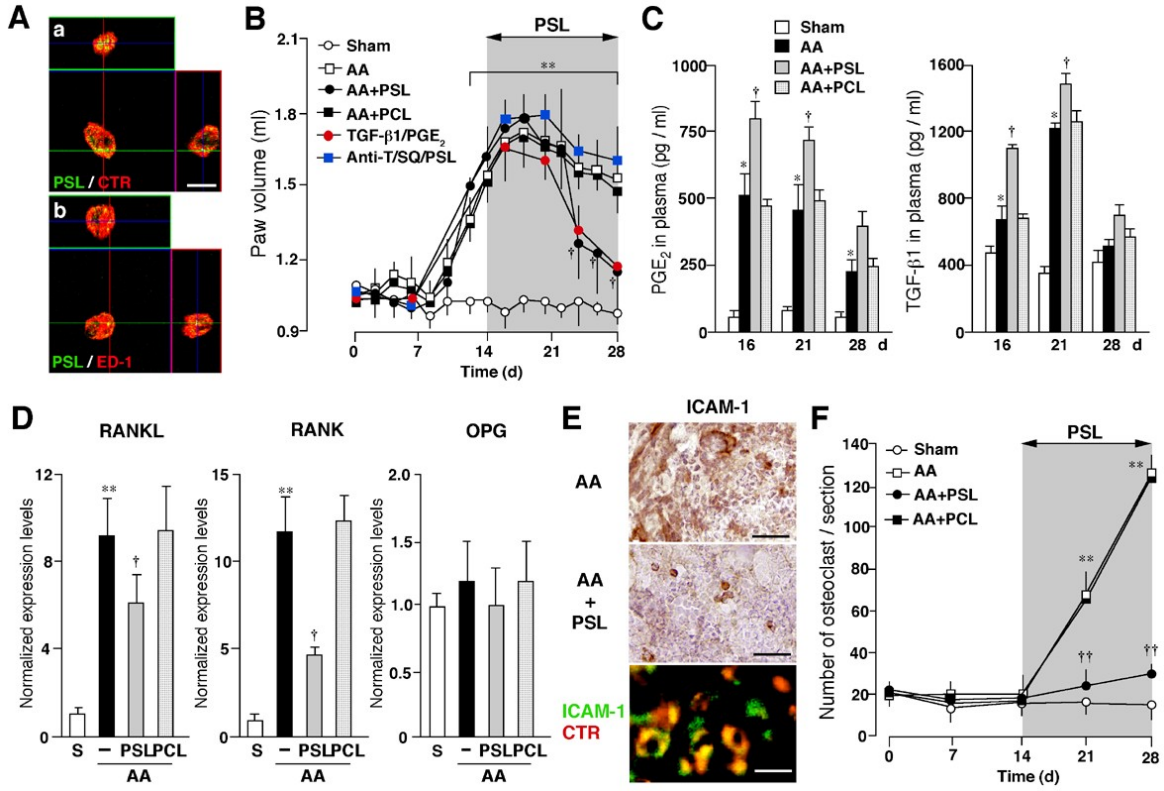

Figure 5 Effects of systemic treatment with PS liposomes (PSL) on osteoclast formation in the AA rats.

A, CLSM images of plan view with two orthogonal cross sectional views clearly showed that NBD-PSL (green) were engulfed by CTR-positive OP cells (red) in the tibia bone marrow of AA rats (*a*). In the peripheral blood of the AA rats (*b*), NBD-PSL (green) localized in ED1-positive mononuclear cells (red) (Scale bar=10 μm). *B*, Effects of PSL and PC liposomes (PCL) on the mean paw volume after CFA injection. *C*, The time course levels of TGF-β1 and PGE_2 in the plasma of the AA rats after systemic treatment with PSL and PCL. *D*, Effects of PSL and PCL on the mean mRNA levels of RANKL, RANK and OPG in skeletal tissues of the AA rats after 7 days treatment. *E*, The immunoreactivity for ICAM-1 in the tibia bone marrow cavities of AA or PSL-treated AA rats (Scale bar=50 μm), and a CLSM image shows that the immunoreactivity for ICAM-1 corresponded with that of CTR in the AA rats (Scale bar=20 μm). *F*,

The effects of PSL and PCL on the mean number of TRAP-positive osteoclasts in the tibia bone marrow cavity in the AA rats. Each symbol and bar represents the mean±SD from 6 rats at each group. The asterisks indicate significant differences between the sham rats and untreated AA rats (**P<0.05, **P<0.01, Student's t-test). The swords indicate a significant difference between the PSL-treated AA rats and untreated AA rats (†P<0.05, ††P<0.01, Student's t-test).

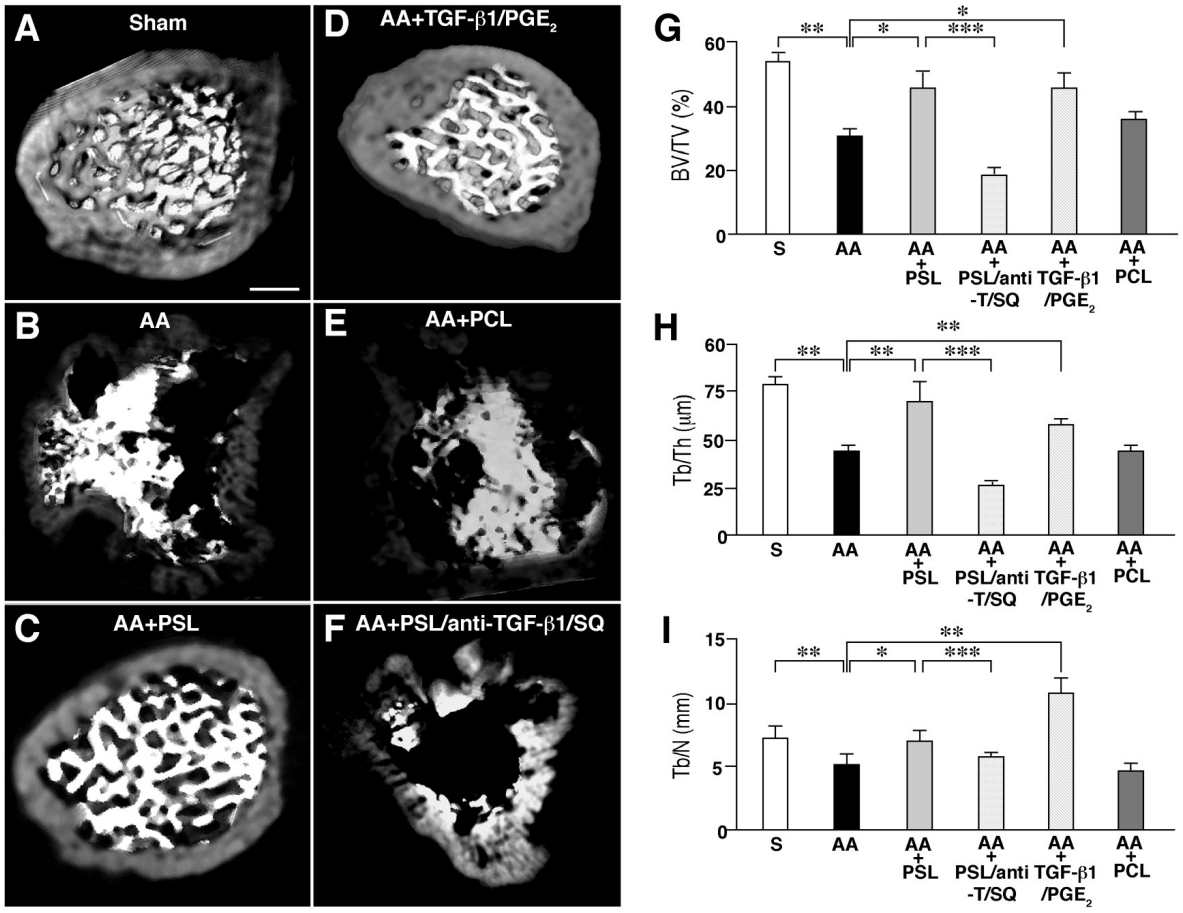

Figure 6 μCT analyses of the effect of PS liposomes (PSL) on the AA-induced trabecular bone loss.

A-C, μCT images of calcaneus in the ankle joints of sham rats (*A*), untreated AA rats (*B*), the PSL-treated AA rats (*C*), the TGF-β1 and PGE_2-treated AA rats *(D)*, the PC liposome (PCL)-treated AA rats (*E*), the anti-TGFβ1 and SQ22536 and PSL-treated AA rats *(F)* at day 14 after the treatments. *G-I*, The mean volume of trabecular bone per unit of metaphysis (BV/TV, G), the mean of trabecular thickness (Tb/Th, H) and the mean of trabecular numbers (Tb/N,I) in sham rats (S), untreated AA rats (AA), PSL-treated (AA+PSL), PCL-treated (AA+PCL), TGF-β1with PGE_2-treated (AA+TGF-β1/PGE_2), anti-TGFβ1 with SQ22536 and with PSL-treated (AA+PSL/anti-TGFβ1+SQ) AA rats. Each column and bar

represents the mean±SD from 6 rats at each group. The asterisks indicate significant differences between the values (*P<0.05, **P<0.01, Student's t-test). The swords indicate a significant difference between the PSL-treated AA rats and untreated AA rats (†P<0.05, ††P<0.01, Student's t-test).

Discussion

The major finding of this study is that PS liposomes inhibit the osteoclastogenesis and AA-induced trabecular bone loss in rats. This is the first report to clarify the effects of PS liposomes on osteoclasts. However, the effects of PS liposomes on macrophages and dendritic cells, which are differentiated from the common myeloid precursors with osteoclasts, have been described elsewhere (18, 19). The current findings are consistent with a recent observation that PS liposomes inhibit the maturation of myeloid dendritic cells (17).

TGF-β1 and PGE_2 secreted from PS liposomes-engulfed OP cells were thought to be closely associated with the inhibitory effects of PS liposomes on the osteoclastogenesis and AA-induced bone loss for two reasons. Firstly, addition of either TGF-β1 or PGE_2 alone significantly inhibited osteoclastogenesis (the formation of TRAP-positive MNCs) in both the rat culture systems at the concentration of 500 pg/ml. Secondly, the inhibitory effect of PS liposomes on the osteoclastogenesis was significantly reversed by an antibody against TGF-βRII, the receptor for the signaling of response to TGF-β1 (43). The effect of PS liposomes on the osteoclastogenesis was also significantly antagonized by SQ22536, an adenylate cyclase inhibitor, thus suggesting the involvement of EP2 and/or EP4 receptors that are coupled to adenylate cyclase (44). The substantial concentration of TGF-β1, which alone could suppress the osteoclastogenesis in BM and OP cell cultures, was estimated to be 800 pg/ml and 650 pg/ml, respectively, because of the relatively high basal level of TGF-β1 in the culture medium (i.e. 300 pg/ml in BM cells, 150 pg/ml in OP cells). On the other hand, the substantial concentration of PGE_2, which alone could suppress the osteoclastogenesis, was estimated to be 650 pg/ml and 580 pg/ml in BM and OP cell cultures, respectively, because of relatively high basal level of PGE_2 in the culture medium (i.e. 150 pg/ml in BM and 80 pg/ml OP cells). PS

liposome-induced secretion of either TGF-β1 or PGE_2 in the culture medium did not reach the concentration to inhibit the osteoclastgenesis in BM and OP cell cultures. Either TGF-β1 or PGE_2 alone at the concentration of 50 pg/ml had no effect on the osteoclastogenesis, however their combine treatment significantly suppressed it. Therefore, it is reasonable to consider that PS liposomes inhibited the osteoclastogenesis by a synergistic effect of TGF-β1 and PGE_2. This can explain the reason why anti-TGF-β1 Ab alone or by SQ22536 alone can suppress the PS liposome-induced inhibitory effect on the osteoclastogenesis. The effects of TGF-β1 and PGE_2 on bone metabolism are still matters of controversy. TGF-β1 enhances osteoclastogenesis even at low concentrations (less than 100 pg/ml), while inhibits it at a high dose (e.g. 2 ng/ml) (34, 35). Although PGE_2 is generally believed to stimulate osteoclastogenesis in murine cultured cells at a relatively high concentration (36-38), PGE_2 also inhibit osteoclastogenesis in human and rat culture systems (39-44). Therefore, it is conceivable that their effects depend on experimental conditions including the cell types, species and the concentrations. Additional experiments are necessary to elucidate the effect of PS liposomes on the human osteoclast formation.

PS liposomes could be phagocytosed by OP cells, thus inhibiting osteoclastogenesis. These results indicate that PS liposomes affect the destiny of OP cells by generating TGF-β1 and PGE_2, which may act in an autocrine manner. On the other hand, PS liposomes also inhibit osteoclastogenesis from BM cell cultures. This suggests that PS liposomes also affect the functions of osteoblasts and stromal cells in paracrine manner, because they have receptors for both TGF-β1 and PGE_2 (45, 46). PS liposomes activate p44/p42 extracellular signal-regulated kinase (ERK) but not p38 mitogen-activated protein kinase in primary cultured rat microglia (16) and macrophages (15). In addition, the PS liposomes-induced PGE_2 production is mediated by COX-1 and its functionally coupled up-regulated terminal prostaglandin E synthases (PGESs), especially

mPGES-2 (16). Furthermore, bafilomycin A_1, a specific inhibitor of vacuolar-type H^+-ATPase, almost completely inhibited PS liposome-induced PGE_2 generation, thus suggesting the involvement of lysosomal proteolytic functions in the PGE_2 generation following phagocytosis of PS liposomes. It is reasonable to consider that PS liposomes also activate such unique intracellular pathway in OP cells to generate TGF-β1 and PGE_2. Further studies to clarify the intracellular signaling pathways activated after phagocytosis of PS liposomes are now in progress.

The down regulation of both RANKL and RANK may be a potential mechanism for the inhibitory effect of PS liposomes on rat osteoclastogenesis, because the RANKL/RANK pathway plays essential roles in differentiation and the fusion of the precursors into mature osteoclasts (20-22). The disruption of either the RANKL or RANK gene causes severe osteopetrosis in mice, with very few osteoclasts in the skeletal tissues (21, 23). In addition, the RANKL/RANK pathways are primarily involved in trabecular bone loss in the AA rats (24). In the present study, PS liposomes significantly decreased the protein amounts of RANKL in BM cells and RANK in the rat bone marrow cultures. Furthermore, TGF-β1 inhibited the RANK expression in OP cells as reported previously (47-49), PGE_2 suppressed the RANKL expression in BM cell cultures in our rat culture system, thus suggesting that PS liposomes affect the proximal signaling of osteoclastogenesis. PS liposomes inhibited the formation of mature osteoclasts but not that of OP cells, thus suggesting that PS liposomes may consequently inhibit cell-to-cell contact and/or cell fusion during osteoclastogenesis. These observations prompted us to further examine the effect of PS liposomes on the expression level of ICAM-1 and CD44, which are the important adhesion molecules for the fusion of OP cells during differentiation (25-27). Consistent with published reports (26, 27, 50), the ICAM-1 and CD44 are expressed on the OP cells. Furthermore, PS liposomes decreased the ICAM-1 and CD44

expression on osteoclasts precursors at the early stage of osteoclastogenesis in rat BM cell cultures. Therefore, another potential mechanism underlying the inhibitory effect of PS liposomes on the osteoclastogenesis is the inhibition of the OP cells fusion through the reduction of the ICAM-1 and CD44 expression. Moreover, TGF-β1 and PGE_2 reduced the ICAM-1 and CD44 expression, respectively, in OP cell cultures during the early stage of osteoclastogenesis. These are in line with the previous finding that both TGF-β1 and PGE_2 inhibit ICAM-1 expression in monocytes (51-54). Taken together, these observations strongly suggest that TGF-β1 and PGE_2 are major causative factors for PS liposomes-induced inhibition of the rat osteoclastogenesis through reducing the expression of RANK, RANKL, ICAM-1 and CD44 at the early stage of osteoclastogenesis.

In parallel with the *in vitro* experiments, the effects of PS liposomes were further examined on the bone destruction associated with AA, which is widely used in research of inflammation and bone destruction (55, 56). We have noted previously that the inflammation of the synovial tissues peaks at 14 to 21 days after CFA injection, and the trabecular bone loss in the bone cavities occurs thereafter (31, 32). To focus on the effects of PS liposomes on AA-induced trabecular bone loss, systemic treatment with PS liposomes was started at 14 days after CFA injection, when the inflammation is established without bone destruction in the ankle joints. The following sequential events were observed after systemic treatment of PS liposomes in the AA rats: (1) phagocytosis of PS liposomes by OP cells in the bone marrow and monocytes in blood, (2) a significant increase in the plasma level of both TGF-β1 and PGE_2, (3) a significant decrease in AA-induced elevated expression of RANKL, RANK, ICAM-1 in the skeletal tissues with the decrease in TRAP-positive osteoclast formation, (4) a significant inhibition of the AA-induced trabecular bone loss. Furthermore, systemic treatment with TGF-β1 and PGE_2 together significantly

reduced the AA-induced trabecular bone loss, and blocked the TGF-β1 and PGE_2 by systemic treatment with anti-TGF-β1antibody and SQ22536 completely reversed the inhibitory effects of PS liposome the AA-induced trabecular bone loss. These *in vivo* findings further support the hypothesis that PS liposomes inhibit osteoclastogenesis by generating TGF-β1 and PGE_2. The deficit of osteoclastogenesis may further lead to the inhibition of AA-induced bone loss. Moreover, in addition to the regulation of osteoclastic bone resorption, TGF-β1 and PGE_2 are also the potent stimulators of osteoblastic bone formation. In this present study, we confirmed that systemic treatment with TGF-β1 and PGE_2 markedly improved the AA-induced decrease of trabecular bone network, especially in trabecular numbers. Those results were accordance with the previous reports, which showed that local subcutaneous injection of either TGF-β1 or PGE_2 increases the activity of osteoblasts to cause the bone formation (57, 58). Therefore, increased TGF-β1 and PGE_2 levels at the early stage after treatment with PS liposomes contribute not only to the prevention of trabecular bone loss, but also to the facilitation of trabecular bone formation in the AA rats.

In conclusion, the current findings strongly suggest that PS liposomes potently inhibit rat osteoclastogenesis and AA-induced trabecular bone loss in rats by generating TGF-β1 and PGE_2.

It has been demonstrated that PS liposome can be phagocytized by osteoclast precursor and directly inhibit the osteoclastogenesis and the inflammatory bone loss in AA rat by stimulating the secretion of TGF-β1 and PGE_2. Since PS-dependent phagocytosis of apoptotic cells is believed to trigger the secretion of anti-inflammatory cytokines and restrains that of pro-inflammatory cytokines from macrophages, it is reasonable to speculate that infiltrated macrophages can undergo a phenotypic change from pro- to anti-inflammatory cells after phagocytosis of PS liposomes. This phenotypic change likely has important consequences on inflammatory bone loss, because pro-inflammatory cytokines are strong inducers of the RANKL and RANK, which play essential roles in differentiation and the activity of osteoclasts.

Thus, in the following study, the effects of PS liposomes on the phenotypic changes of infiltrated macrophages, which were considered indirectly inhibiting osteoclastogenesis during inflammatory bone loss, were elucidated.

Chapter II:
Phosphatidylserine-Containing Liposomes Suppress Inflammatory Bone Loss by Ameliorating the Cytokine Imbalance in the Ankle Joints of Adjuvant Arthritic Rats

Introduction

Apoptosis is known to be associated with the resolution of inflammation by regulating the release of cytokines (11, 13, 59, 60). Accumulating evidence shows that exposure of PS plays a central role in the recognition and phagocytosis of apoptotic cells by phagocytes (6, 9, 10). PS-dependent phagocytosis of apoptotic cells is believed to trigger the secretion of anti-inflammatory cytokines and restrains that of pro-inflammatory cytokines from macrophages (12, 61) and dendritic cells(14, 62). Furthermore, PS liposomes can promote the resolution of inflammation *in vivo* (13, 63, 64).

In the first part of present study, it has demonstrated that PS liposome can be phagocytized by osteoclast precursor to directly inhibit osteoclastogenesis depend on the secretion of TGF-β1 and PGE_2. The strong inhibition of osteoclastogenesis consequently contributed inhibition of the inflammatory bone loss in AA rats (65). However, it is also reasonable that infiltrated macrophages can undergo a phenotypic change from pro- to anti-inflammatory cells after phagocytosis of PS liposomes. This phenotypic change likely has important consequences on inflammatory bone loss, because pro-inflammatory cytokines are strong inducers of the RANKL and RANK, which play essential roles in differentiation and the activity of osteoclasts (56).

Among pro-inflammatory cytokines, IL-1β is a master regulator of inflammation and inflammatory bone loss, because it can induce other pro-

inflammatory cytokines (66, 67). Recently, much attention has been paid to IL-17 as a crucial cytokine for inflammatory osteoclastic bone loss because of its marked induction of RANKL (68). Indeed, high levels of IL-1β and IL-17 are found in the plasma and synovial tissues of RA patients, and combined blockade of IL-1β and IL-17 receptors significantly inhibited the rheumatoid arthritic osteoporosis (69). Among anti-inflammatory mediators, including TGF-β1 and PGE_2, IL-10 is known as the strongest feedback mediator of inflammatory bone loss (70, 71).

In this part of the present study, we attempted to elucidate the effects of PS liposomes on the phenotype of infiltrated macrophages in the skeletal tissues of ankle joints of AA rats, an animal model of RA (72, 30, 32). We have herein demonstrated that infiltrated macrophages underwent a phenotypic change from IL-1β-producing to IL-10-producing cells. This PS liposome-induced phenotypic change of infiltrated macrophages also contributes to the inhibition of AA-induced trabecular bone loss through the inhibition of RANKL/RANK expression and the subsequent osteoclastogenesis.

Materials and Methods

Reagents

Dulbecco's Modified Eagle's Medium (DMEM) was purchased from Sigma (Saint Louis, MI). The mouse monoclonal anti-ED1 antibody was from BMA (Augest, Switzerland); goat polyclonal anti-IL-10, anti-IL-1β, rabbit polyclonal anti-IL-17, anti-p-IκBα, mouse monoclonal anti-NF-κB antibodies were obtained from Santa Cruz Biotechnology Inc. (Santa Cruz, CA). Rabbit polyclonal anti-p38, anti-p-p38, anti-ERK and anti-p-ERK antibodies were form Cell Signaling Technology (Beverly, MA).

Heat-inactivated *Mycobacterium butyricum*, mineral oil, TGC, FBS, PS, PC, NBD-labeled PS, and NBD-labeled PC were same with the former.

Liposomes

Same with that of chapter I

Systemic PS liposomes Treatment for Adjuvant Arthritic Rats and Samples Preparation

The method of systemic liposomes treatment and samples preparation were almost same with that of the chapter I. what different were that, in this study, the systemic liposome treatment was start at day 10 after CFA injection and samples were taken at day 4, 11 or 18 after PSL or PCL treatment. No TGF-β1 and PGE_2 treatment were done in this time.

Preparation of Peripheral Blood Monocytes

Rats were anesthetized with sodium pentobarbital (30 mg/kg, i.p.) at day 7 after PS liposomes treatment. The peripheral blood (PB) was collected from the inferior vena cava of rats and supplemented with novo-heparin (5units/ml, Mochida Pharmaceutical CO., LTD, Tokyo Japan). PB was carefully layered onto HISTOPAQUE 1083 （ Sigma, Missouri USA） and then centrifuged at 400×g for 30 minutes at 24˚C. The mononuclear cell layer was taken out carefully after transfer the opaque interface; wash twice with PBS and centrifugation at 250xg for 10 minutes at 24˚C. Cells suspended in DMEM were incubated at 37˚C in a 5% CO_2 atmosphere for 3 h. The purity of monocytes was more than 98% of the adherent cells which was determined by the

immunostaining of ED1 after removing the non- adherent cells. The adherent monocytes were cultured for another 24 h for further assays.

Real-Time quantitative RT-PCR Analysis

The method of Real-Time quantitative RT-PCR analysis was same with that of Chapter I. The total RNA from ankle join tissue and PB monocytes was extracted.

Primer sequences were as follows: IL-10: 5'-GAAGCTGA-AGACCCTC-TGGATACA-3' and 5'-CCTTTGTCTTGGAGCTTATTAAAATCA- 3'; IL- 1β: 5'-CCTGTGGCCTTGGGCCTCAA-3' and 5'-GGTGCTGATGTACC-AGTTGGG-3'; IL-17: 5'-TTCTCCAGAACGTGAAGGTC-3' and 5'-GGACAA- TAGAGGAAACGCAG-3'. RANKL, RANK, and OPG were same with the former.

μCT Analysis

The ankle joints of sham, AA rats and the AA rats at day 1 after the treatment in each group (n=6) were examined using ScanXmate-E090S40 in vivo (Comscantecno, Co. Ltd, Kanazawa, Japan). Briefly, rat paws were scanned, the tibia, talus and calcaneus in the ankle joints were examined by three-dimension surface rendering with a common threshold, and were optimized using histomorphometric techniques (GEMS MicroView). Because the trabecular bone loss within the tibia and talus in the AA rats was too severe to quantify, calcaneuses were used for the bones qualitative analyses. The parameters of trabecular bone in each group were analyzed using TRI/3D-BON software program (Ratoc System Engineering Co. Ltd. Tokyo, Japan).

Preparation of Peritoneal Macrophages

Rat peritoneal macrophages were collected with DMEM medium 4 days after the injection of TGC (4.05 mg/kg, i.p.). The collected cells were washed twice with DMEM, containing 4500 mg glucose/L, L-glutamine, $NaHCO_3$ and pyridoxine, HCL (Sigma, D5796) and plated on plastic tissue culture dishes (2×10^6 cells). After incubation at 37ºC in a 5 % CO_2 atmosphere for 3 h, the nonadherent cells were removed by washing the dishes three times with DMEM medium. The cell pattern was determined by cell morphology analysis with a light microscope. The total cells (95 % macrophages) were incubated at 37 ºC/5 % CO_2.

Western Blotting

The macrophages were stimulated by LPS (10 ng/ml) and treated with PS liposomes (100 μM) at the same time. The PS liposome-treated or untreated macrophage extracts were prepared with cell lysis buffer as described previously.[13] A Western blots analysis was performed with the following antibodies: rabbit polyclonal anti- p38 MAPK (1:500 dilution), anti-p-p38 MAPK (1:500 dilution); anti- ERK (1:500 dilution), or anti-p-ERK (1:500 dilution).Bands were detected by the enhanced chemiluminescence detection system (ECL kit, Amersham Bioscience, Uppsala, Sweden) and quantified with an image analyzer FLA3000 (Fuji Photo Film, Tokyo, Japan). Values of p-p38 and p-ERK were normalized to total p38 and ERK values.

ELISA

The macrophages were activated by LPS (10 ng/ml) for 1 h, then treated

with PS liposomes (100 μM) for another 3 h. Supernatants of the cultured cells were collected, and the release of the IL-10 and IL-1β were measured using IL-10 and IL-1β ELISA kits (R&D, Minneapolis, MN). The assay was performed according to the manufacturer's directions. The absorbence at 450 nm was performed using a microplate reader (Bio-Rad Laboratories. Hercules, CA).

Immunohistochemistry and Histological Analysis

The sections of ankle joints from sham, AA and the PS liposome-treated AA rats were blocked with 10 % normal donkey serum, and were incubated with goat anti-IL-10, anti-IL-1β, anti-IL-17, mouse anti-ED1 and anti-W3/25 antibodies for 18 h at 4 ˚C. After incubating with a biotinylated anti-goat or anti-rabbit or anti-mouse IgG (1:200, Jackson Immunoresearch Lab. Inc., West Grove, PA) for 2 h at 24 ˚C, the sections were incubated with peroxidase-conjugated streptavidin (1:300, Dako Japan, Kyoto, Japan) for 30 min at 24 ˚C. The peroxidase was developed using 3, 3'-diaminobenzidine, and Mayer's hematoxylin as a counterstain. The normal goat, mouse or rabbit antibodies, which were substituted for primary antibodies, were used as negative controls. The immunoreactive cells were counted under a light microscope using the ×40 objective and ×10 ocular lenses in three areas per section. Histological Analysis was preformed by hematoxylin-Eosin (H-E) and TRAP staining (TRAP kit, Sigma-Aldrich).

Immunofluorescent Staining

To detect the cellular source of the cytokines in the ankle joints tissues, the sections were treated with 10 % donkey serum for 1 h at 24 ˚C, and then were incubated with each primary antibody for 18 h at 4 ˚C. The primary antibodies

were goat polyclonal anti-IL-10, anti-IL-1β rabbit polyclonal anti-p-p38, anti-p-ERK and anti-p-IκBα mixed with mouse monoclonal ED1 or anti-W3/25 antibodies. After washing with PBS, the sections were incubated with a mixture of FITC-conjugated and rhodamine-conjugated secondary antibodies for 1 h at 24 ˚C. After washing, the sections were mounted in the anti-fading medium Vectashield (Vector Laboratory). The phagocytosis of PS liposomes by macrophages *in vivo* and PB monocytes *in vitro* was also examined. *In vivo*, after 6 h of systemic treatment with NBD-labeled PS liposomes (5 mg/kg) or NBD-labeled PC liposomes (5 mg/kg) in AA rats, the animals were intracardially purfused with 2% PFA, and the ankle joints were removed and immersed in the same fixative for 12 h at 4 ˚C. After immersing in 30% sucrose in PBS for 2 days, samples were embedded in an optimal cutting temperature compound (Sakura Finetechnical Co., Ltd., Tokyo, Japan). Serial coronal frozen sections (10 μm) were prepared for immunohistochemistry. *In vitro*, NBD-labeled PS liposomes (100 μM) or NBD-labeled PC liposomes (100 μM), were applied to cultured PB monocytes on chamber slides (Nalge Nunc International, Rochester, NY), and the cells were collected after 4 h. The cells were fixed with 2% PFA for 30 min at 24 ˚C. After incubation with 10% donkey serum, the samples were incubated with mouse anti-ED1 IgG (1:200) for 18 h at 4 ˚C. After washing with PBS, the slides were incubated with rhodamine-conjugated donkey anti-mouse IgG for 30 min at 24 ˚C. The slides were mounted with Vectashield (Vector Laboratory). The samples were examined with a confocal laser scanning microscope, LSM510MET (Carl Zeiss, Jena, Germany).

Statistical Analysis

Data are expressed as means ± SD. The significant differences between groups were determined with student's *t*-test.

RESULTS

The Effects of PS liposomes on the Paw Swelling, bone destruction, Trabecular Bone Loss, and Expression of RANKL/RANK in the Ankle Joints of AA Rats

The paw volume increase of AA rats occurred in two stages: an acute inflammation stage from days 10-21 after CFA injection, and the chronic bone/joint destruction stage thereafter (Figure 7A). The paw volume of AA rats did not return to the control levels (Figure 7A, C). The CFA-induced clinical symptoms were similar to those in chapter I and our previous studies (27, 28, 29). To focus on the effects of PS liposomes on AA-induced inflammatory bone loss, systemic treatment with PS liposomes was begun 10 days after CFA injection, when the inflammation was established without bone destruction in the ankle joint. Treatment with PS liposomes for 18 days significantly reduced the paw volume and the infiltrated inflammatory cells in the synovial tissues of ankle joints of AA rats at the chronic stage without affecting it at the acute stage (Figure 7A-C).According to the three-dimension surface rendering μCT analysis, the bone in the ankle joint including the tibia, talus and calcaneus in AA rats was markedly destructed in comparison to the sham rats (Figure 7D). The analysis of the parameters of trabecular bone was conducted in the calcaneus, because the trabecular bone losses within the tibia and talus in AA rats were too severe to quantify 28 days after CFA injection. Significant decrease in the BV/TV in AA rats was as similar as that of chapter I. Furthermore, numerous of TRAP-positive osteoclasts were detected in the tibia bone cavity of AA rats (Figure 7E). Treatment with PS liposomes significantly promoted the recovery of the AA-induced paw volume increase and the inflammatory cells infiltration in the synovial tissues (Figure 7A-C) and bone destruction (Figure

7D, E). However, PC liposomes had no effect on the paw volume of AA rats at any stage (Figure 7A).

The expression of RANKL, RANK and OPG were next examined, because these molecules play essential roles in trabecular bone loss in AA rats. The mean mRNA levels of RANKL and RANK were significantly increased in AA rats in comparison to sham rats, and treatment with PS liposomes for 18 days significantly decreased the AA-induced increased mean mRNA levels of both RANKL and RANK in the ankle joints of AA rats (Figure 7F,G).The mean mRNA level of OPG was unchanged after CFA injection, and PS liposomes had no effect on the expression of OPG of AA rats (Figure 7H). These observations indicated that treatment with PS liposomes significantly inhibited AA-induced trabecular bone loss by inhibiting RANKL/RANK expression.

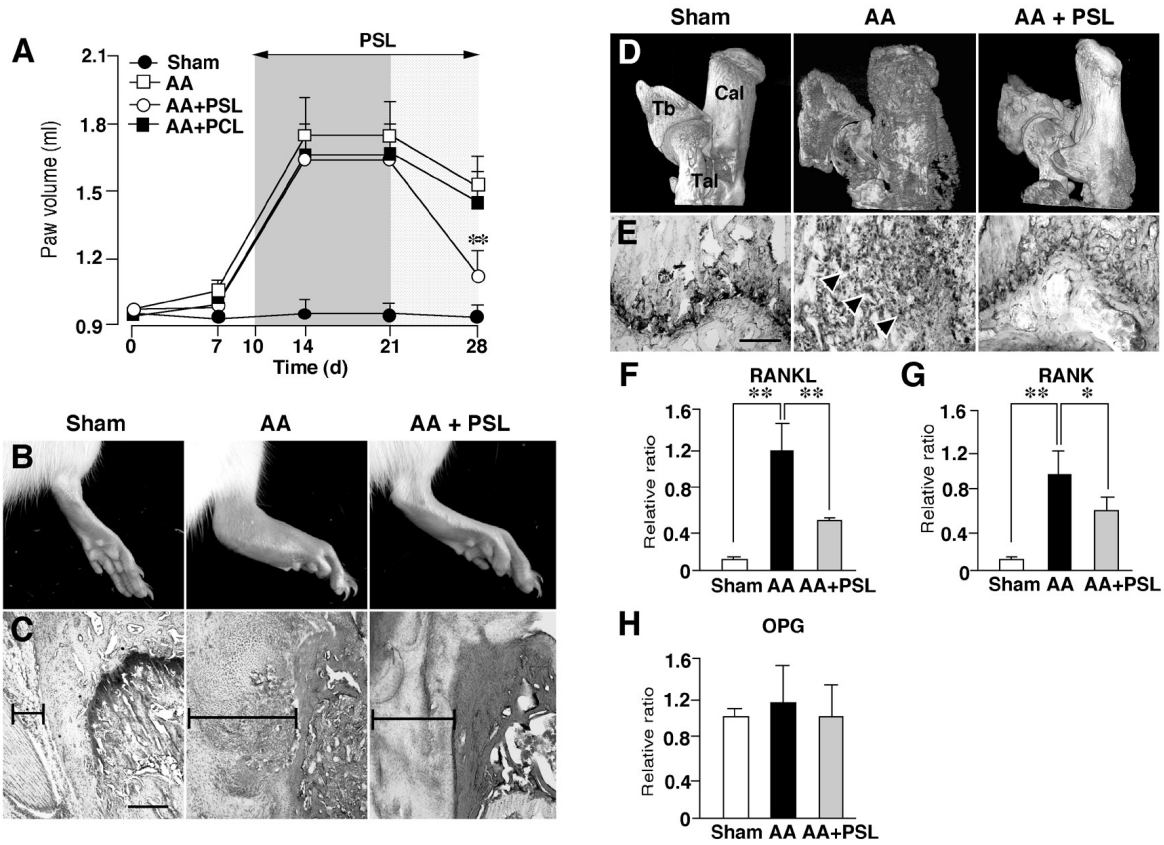

Figure 7. Effects of systemic treatment with PS liposomes (PSL) on paw swelling, trabecular bone loss, and expression of RANKL/RANK in the ankle joints of AA rats.

(A) The time course of the mean paw volume of AA rats after CFA injection. Each symbol and bar represents the mean ± SD from 6 rats at each group. Sham: sham rats, AA: AA rats, AA+PSL: PSL-treated AA rats, AA+PCL: PCL-treated AA rats. The asterisks indicate significant differences between AA and AA+PSL (*P<0.05, **P<0.01, Student's t-test). (B) Photographs showing the macroscopic appearances of ankle joints, (C) H-E staining of synovium of ankle joints. (D) Photographs showing the three-dimension outer surface of bones in the ankle joints, including tibia (Tb), talus (Tal) and calcaneus (Cal) according to the CT

analyses. (E) TRAP staining of bone cavity of epiphyseal of tibia, it is noted that numerous of TRAP positive mature osteoclasts in the AA rats (arrow heads). The mean mRNA levels of RANAL (F), RANK (G) and OPG (H) in the ankle joints in AA. Each column and bar represents the mean ± SD from 3 rats at each group. The asterisks indicate significant differences between these values (*P<0.05, **P<0.01). Scale bar = 50 μm.

Effects of PS liposomes on the Pro- and Anti-inflammatory Cytokine Production by the Infiltrated Inflammatory Cells in the Ankle Joints of AA Rats

At 6 h after intramuscular treatment, large granular aggregates of PS liposomes (green) were encircled by lysosomal membranes stained with the anti-ED1 antibody (red) in the infiltrated macrophages in the synovium of ankle joints (Figure 8A). Interestingly, treatment with PS liposomes significantly reduced the total numbers of either $ED1^+$ macrophages or $W3/25^+$ helper T cells, which are the major infiltrated cells that are involved in the pathological process of RA in AA rats, in the synovium of ankle joints of AA rats at the chronic stage, without affecting their infiltration at the acute stage (Figure 8B).

The failure of PS liposomes to inhibit the infiltration of immune cells into the ankle joints of AA rats at the acute stage led us to examine the effects of PS liposomes on the phenotypic changes of infiltrated macrophages and helper T cells. In comparison with sham rats, the mean mRNA expression levels of IL-10 and IL-1β significantly increased in AA rats at days 14 to 21 after CFA injection (Figure 8C, D). However, IL-17, a major cytokine secreted by helper T cells, was also induced in the ankle joints of AA rats at 21 days after CFA injection (Figure 8E). Systemic treatment with PS liposomes was begun from day 10 after CFA injection. It was noted that treatment with PS liposomes for 4 and 11 days significantly increased the mean mRNA level of IL-10 (Figure 8C). On the other hand, PS liposomes significantly decreased the mean mRNA levels of IL-1β and IL-17 in the ankle joints of AA rats over same periods (Figure 8D, E).

According to the immunochemical analyses, the localization of the cytokines was determined in the synovium of ankle joints at the acute stage of AA rats (Figure 9). The mean number of IL-10-positive cells significantly increased 11 days after treatment with PS liposomes (Figure 9A, B, G).

However, the mean numbers of IL-1β-positive cells and IL-17-positive cells in AA rats were significantly decreased (Figure 9C-F, H, I). No immunoreactivity was observed when normal rabbit IgG, normal goat IgG or normal mouse IgG was substituted for the primary antibodies as negative controls (data not shown). Furthermore, immunoreactivity for both IL-1β and IL-10 was mainly found in $ED1^+$ macrophages (84% and 62%, respectively) and these cytokines were only partially expressed in $W3/25^+$ helper T cells (8% and 18%, respectively) in the synovium of ankle joints at the acute stage of AA rats. We observed immunoreactivity for IL-1β and IL-10 in $ED1^+$ macrophages (43% and 86%, respectively) after treatment with PS liposomes (Figure 9L).

These observations strongly suggested that approximately half of infiltrated macrophages underwent phenotypic change from IL-1β-producing pro-inflammatory cells to IL-10-producing anti-inflammatory cells after the phagocytosis of PS liposomes.

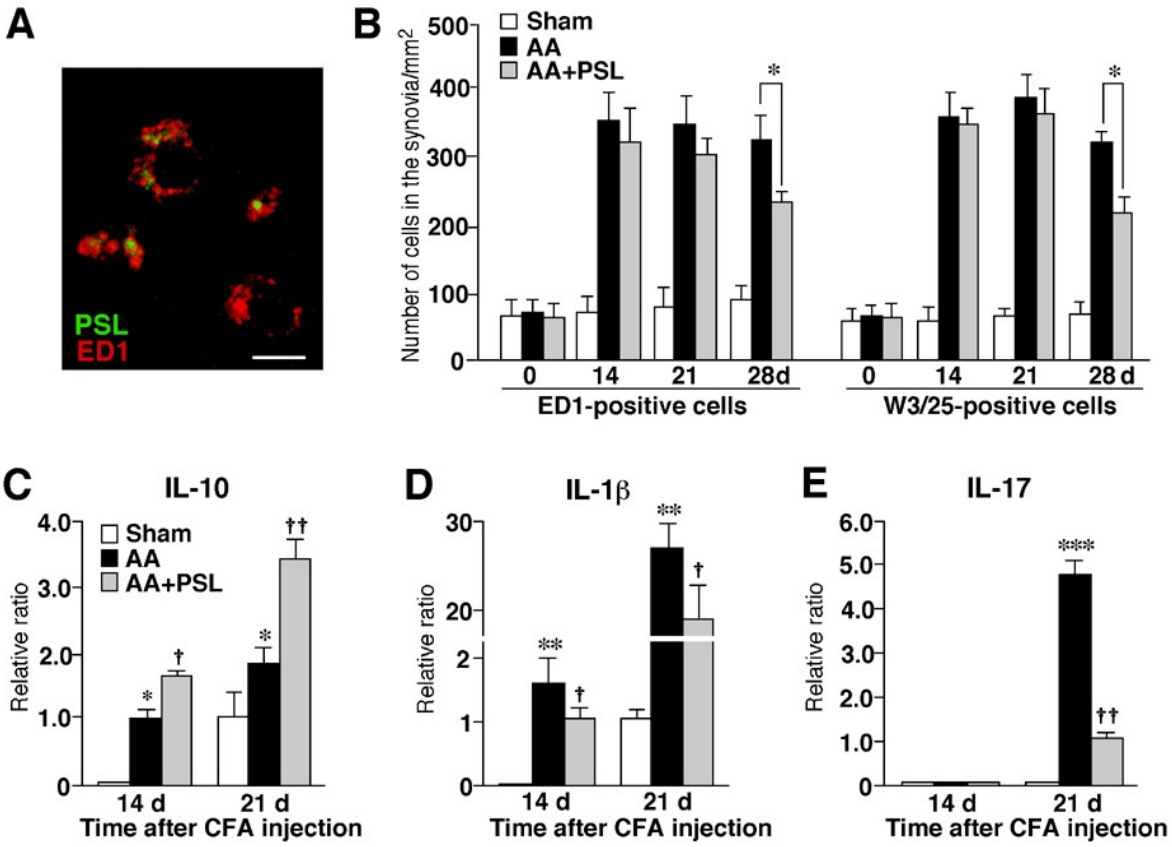

Figure 8. Effects of systemic treatment with PS liposomes (PSL) on the infiltration of macrophages and helper T cells and the expression of IL-10, IL-1β and IL-17 in the ankle joints of AA rats.

(A) Immunofluorescent CLSM images showing NBD-PSL (green) are phagocytozed by ED1$^+$ macrophages (Red) in the synovium of AA. Scale bar = 10 μm). (B) The mean number of ED1$^+$ macrophages and W3/25$^+$ helper T cells in the synovium of ankle joints of Sham, AA and AA+PSL. Each column and bar represents the mean ± SD from 6 rats in each group. The asterisks indicate significant differences between the values (*P<0.05, **P<0.01, Student's t-test). (C-E) The mean mRNA levels of IL-10 (C), IL-1β (D) and IL-17(E) in the ankle joints of AA rats after systemic treatment with PS Liposomes for 4 and 11 days. Each column and bar represents the mean ± SD from 6 rats in each group.

Asterisks indicate significant differences between the sham and AA animals (*P<0.05, **P<0.01, ***P<0.001, Student's t-test), and the swords indicate significant differences between AA and AA+PSL († P<0.05, ††P<0.01, Student's t-test)

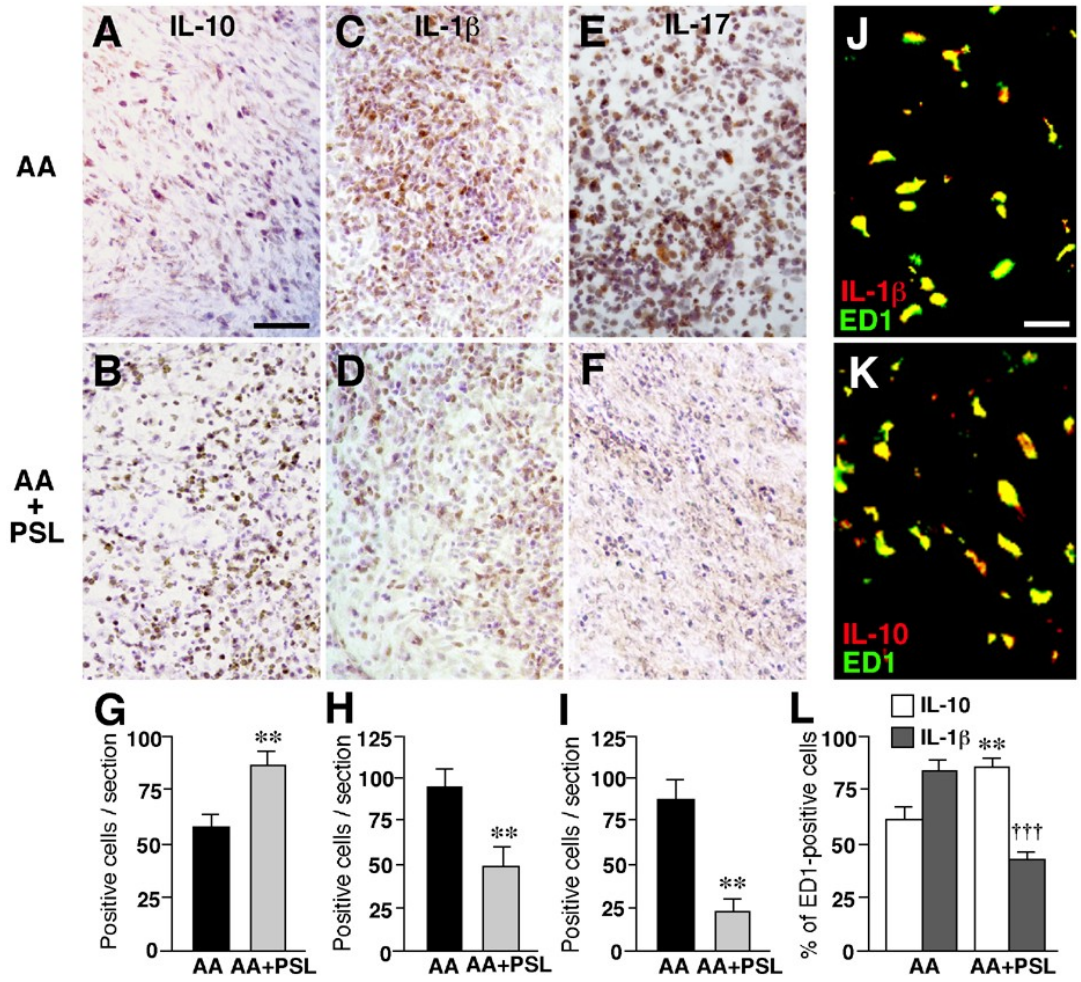

Figure 9. Effects of systemic treatment with PS liposomes (PSL) on the immunoreactivity and localization of IL-10 and IL-1β in the ankle joints of AA rats at 21 days after CFA injection.

(A-F) Immunoreactivities of IL-10 (A, B), IL-1β (C, D) and IL-17 (E, F) in the synovium of ankle joints of AA rats (AA) and PSL-treated AA rats (AA+PSL). (G, H, I) The mean number of positive cells for IL-10 (G), IL-1β (H) and IL-17 (I) in the synovium of ankle joints of AA and AA+PSL. Each column and bar represents the mean ± SD from 6 rats in each group. Asterisks indicate significant differences between AA and AA+PSL (**P<0.01). Scale bar = 20 μm (A-F). (J-K) Identification of IL-1β- and IL-10-expressing cells in the ankle joint in AA. Immunofluorescent CLSM images for IL-1β (red) and ED1 (green)

(J); IL-10 (red) and ED1 (green) (K). (L) The mean ratios of IL-1β and IL-10 in $ED1^+$ macrophages infiltrated in the synovium of ankle joints of AA and AA+PSL. Scale bar = 10 μm (J, K). Each column and bar represents the mean ± SD from 6 rats in each group. Asterisks indicate significant differences between AA and AA+PSL (**P<0.01, ***P<0.001).

PS liposomes Triggered LPS-Activated Macrophages to Anti-inflammatory Phenotype through Regulating MAPKs and NF-κB Activity

To clarify the mechanisms underlying PS liposome-induced phenotypic change of macrophages infiltrated in the ankle joints of AA rats, the effect of PS liposomes on the secretion of IL-10 and IL-1β from LPS-stimulated macrophages was examined, because LPS is a key component of CFA that activates macrophages in AA rats.[31] Although the mean levels of IL-10 and IL-1β in the culture medium were relatively low in the none treated control macrophages, the mean levels were significantly increased after treatment with LPS (Figure 10A, B). PS liposomes significantly increased the IL-10 levels, but significantly decreased the IL-1β levels in the culture medium of LPS-activated macrophages (Figure 10A, B). These *in vitro* results were consistent with the observations from AA rats.

The effects of PS liposomes on the activation of p38 MAPK, ERK and NF-κB, which play key regulatory roles in the cytokine production, were next examined. Upon LPS stimulation, p38 MAPK was activated rapidly afrer 15 to 30 min. In contrast, ERK was activated slowly from 30 min and lasted up to 60 min (Figure 10C). Furthermore, the numerous nuclear translocation of NF-κB was detected at 30 min after treatment with LPS. After treatment with PS liposomes, the mean level of p-p38 MAPK significantly decreased from 15 min to 30 min (Figure 10C, D). However, PS liposomes significantly increased the mean level of p-ERK from 30 to 60 min (Figure 10C, D). Moreover, PS liposomes markedly inhibited the LPS-induced nuclear translocation of NF-κB (Figure 10E).

These observations indicated that PS liposomes inhibited the LPS-induced activation of p38 MAPK and NF-κB, but enhanced LPS-induced activation of

ERK, thus resulting in the shift of the LPS-stimulated macrophages from IL-1β-producing pro-inflammatory cells into IL-10-producing anti-inflammatory cells.

The effects of PS liposomes on the IL-10 and IL-1β production of the PB monocytes in AA rats was further examined, because PB monocytes are the cell source of infiltrated macrophages in the synovium of ankle joints of AA rats. PS liposomes were phagocytosed by ED1-positive PB monocytes of AA rats (Figure 11A). The mean mRNA levels of both IL-10 and IL-1β in the PB monocytes of AA rats were markedly increased in comparison with that in sham rats (Figure 11B, C). Treatment with PS liposomes significantly increased the expression level of IL-10, but significantly decreased that of IL-1β in the PB monocytes of AA rats (Figure 11B, C).

Finally, the effects of PS Liposomes on activation of p38 MAPK, ERK and p-IκBα in the infiltrated macrophages and T cells in the synovium were examined. In AA rats, high expression of p-p38 was detected both in $ED1^+$ macrophages and in $W3/25^+$ helper T cells (Figure 11D, E). In contrast, low expression of p-ERK was detected in $ED1^+$ and in $W3/25^+$ cells (Figure 11D, F). Furthermore, high expression of p-IκBα was also detected both in $ED1^+$ and in $W3/25^+$ cells (Figure 11D, G). After treatment with PS liposomes, the percentages of p-p38 and p-IκBα -positive $ED1^+$ cells were significantly decreased, but that of p-ERK- positive $ED1^+$ cells was significantly increased. However, the percentages of p-p38, p-ERK and p-IκBα -positive in $W3/25^+$ cells were did not significantly changed (Figure 11D-G). These *in vitro* and *in vivo* results indicated that PS liposomes directly target on the infiltrated macrophages in the ankle joints of AA rats.

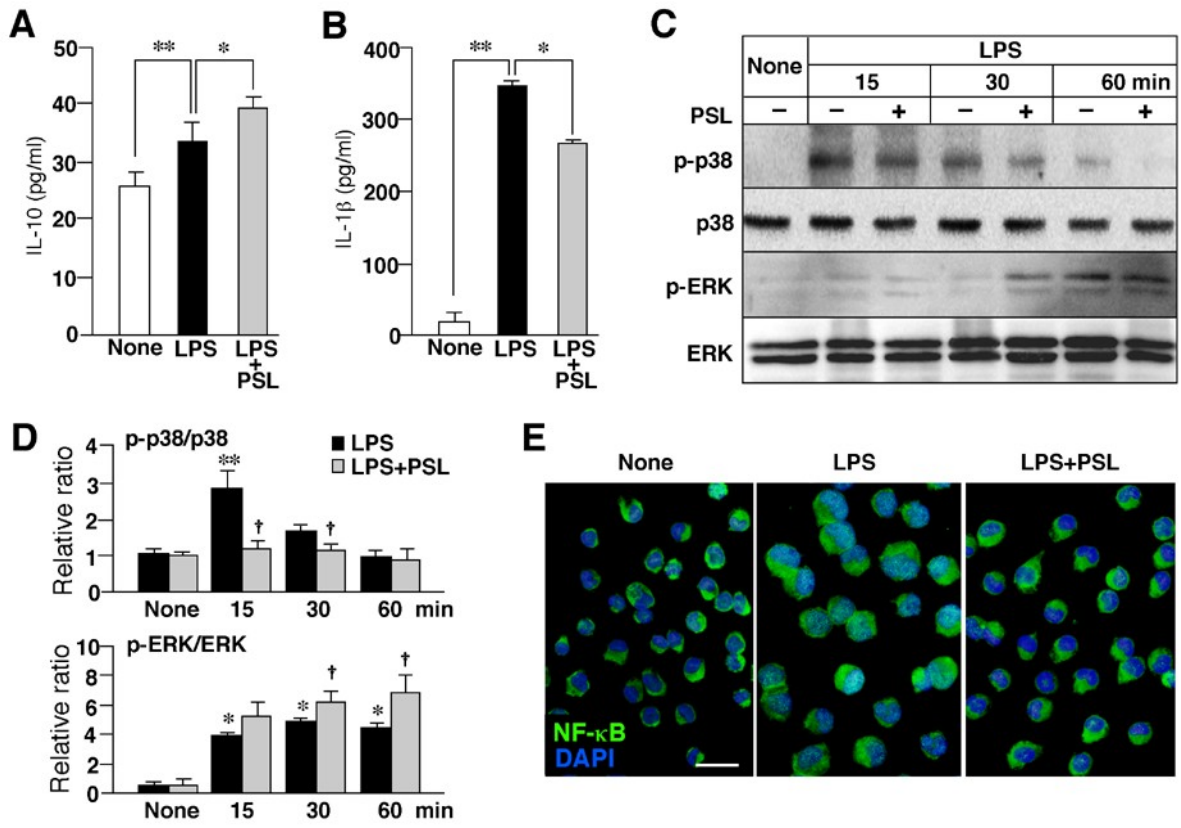

Figure 10. PS liposomes (PSL) trigger LPS-stimulated macrophages to anti-inflammatory phenotype through the down-regulation of p-38 and NFκB activity.

（ A, B ） The mean levels of IL-10 (A) and IL-1β (B) in the culture medium of LPS-stimulated macrophages. None: non-treated cells, LPS: LPS-stimulated cells, LPS+PSL: PSL-treated LPS-stimulated cells. Each column represents the mean of 3 separate experiments. Asterisks indicate significant differences between the values (*P<0.05 **P<0.01). (C) A Western blot analysis of p38 MAPK and ERK in LPS-stimulated macrophages after treatment with PSL. (D). The mean relative ratio of p38 MAPK and ERK activation. Each column represents the mean of 3 separate experiments. Asterisks indicate significant differences between none and LPS-stimulation (*P<0.05 **P<0.01). Swords indicate significant differences between LPS and LPS+PSL (†P<0.05).

(E) Immunofluorescent CLSM images indicating the nuclear translocation of NF-κB (green) in macrophages with DAPI-stained nuclei (blue). None: non-treated cells, LPS: LPS-stimulated cells, LPS+PSL: PSL-treated LPS-stimulated cells.

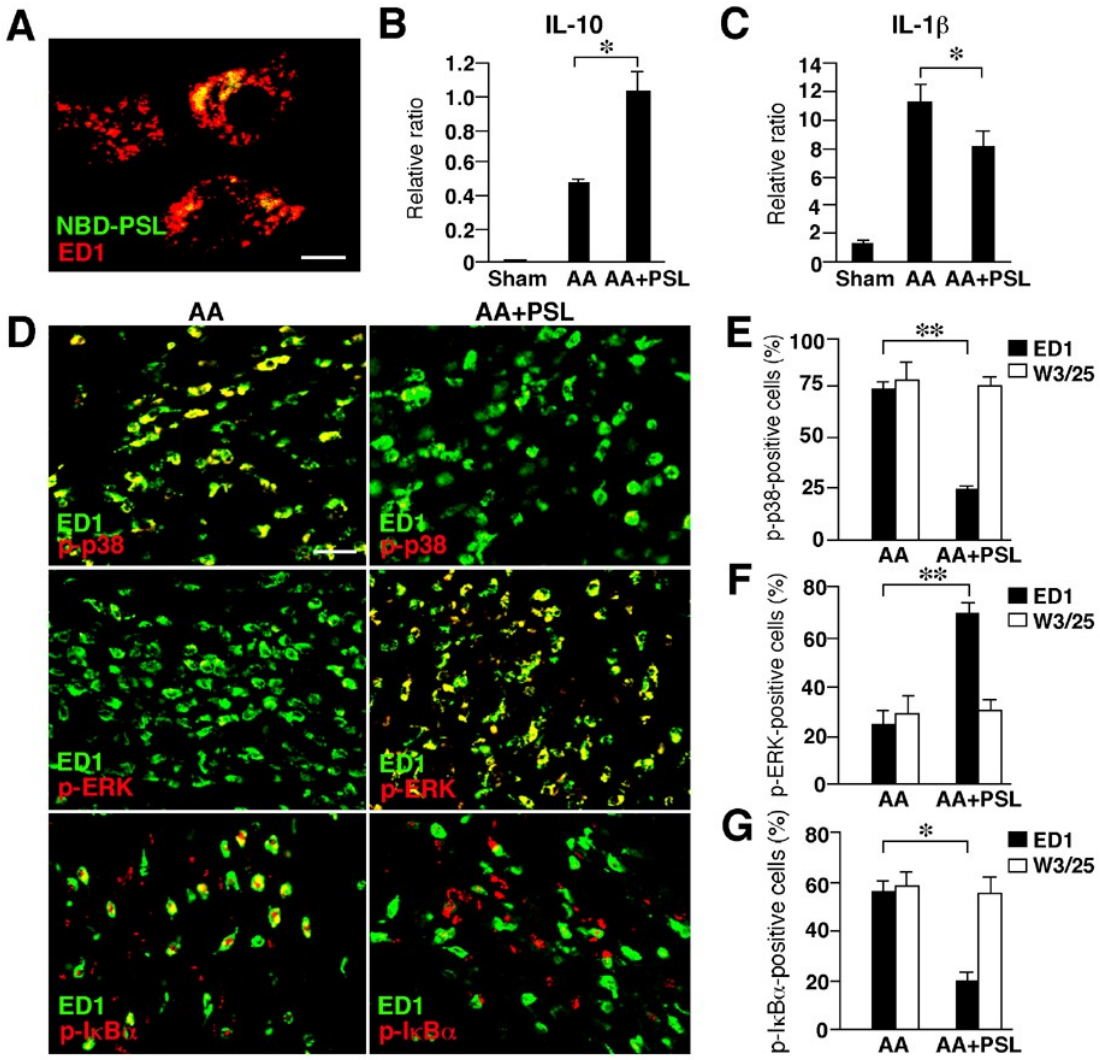

Figure 11. PS liposomes (PSL) trigger the infiltrated macrophages in AA rats to anti-inflammatory phenotype through the down-regulation of p-38 and NFκB activity.

(A) Immunofluorescent CLSM images showing NBD-PSL (green) are phagocytozed by the PB ED1$^+$ monocytes (red) of AA rats (Scale bar = 5μm). (B, C) The mean mRNA levels of IL-10 (B) and IL-1β (C) in the PB ED1$^+$ monocytes of AA rats after systemic treatment with PSL for 7 days. Each column and bar represents the mean ± SD from 6 rats in each group. Asterisks indicate significant differences between the AA and AA+PSL (*P<0.05, **P<0.01,

Student's *t*-test). (D) Immunofluorescent CLSM images for p-p38 (red) and ED1 (green); p-ERK (red) and ED1 (green); p-IκBα (red) and ED1 (green) (Scale bar = 20 μm). (E-G) The mean ratios of p-p38, p-ERK and p-IκBα in the infiltrated $ED1^+$ macrophages and $W3/25^+$ helper T cells in the synovium of ankle joints of AA and AA+PSL. Each column and bar represents the mean ± SD from 6 rats in each group. Asterisks indicate significant differences between AA and AA+PSL (*P<0.05, **P<0.01, Student's *t*-test).

DISCUSSION

The major finding of the current study was that PS liposomes inhibited the AA-induced trabecular bone loss partially through the phenotypic change of infiltrated macrophages from IL-1β-producing pro-inflammatory cells to IL-10-producing anti-inflammatory cells. To the best of our knowledge, this is the first report to address the effect of PS liposomes on the phenotypic changes of macrophages that had infiltrated into the ankle joints of AA rats during inflammatory bone loss.

Pro-inflammatory cytokines produced by macrophages and helper T cells, the major infiltrated cells in the synovium of joints, play pivotal roles in the pathological process of RA (74, 75). AA, an animal model of RA, is widely used for studies of both inflammation and bone loss (56, 76), because AA rats show unique sequential pathological processes. In the acute stage, numerous macrophages and helper T cells infiltrate into the synovium, but, bone loss is not detected. In the chronic stage, trabecular bone loss occurs, and the number of infiltrated macrophages and helper T cells declines (30, 31). In this study, the expression levels of IL-1β and IL-17 were markedly elevated in the ankle joints during the acute stage in AA rats. It was also noted that IL-1β increased prior to the increased levels of IL-17. This was consistent with the fact that IL-1β is essential for promoting Th17 cell differentiation and IL-17 production by the differentiated Th17 cells (77). The expression level of IL-10 also significantly increased during the same period. Treatment with PS liposomes significantly decreased the IL-1β and IL-17 levels, and also significantly increased the IL-10 levels. It was considered that IL-10 secreted from macrophages after phagocytosis of PS liposomes can inhibit IL-1β production and the differentiation of Th17 cells, thus resulting in a decrease in the IL-17 levels (78). This PS liposome-induced phenotypic change of infiltrated macrophages also

contributed to the inhibition of AA-induced trabecular bone loss through the inhibition of RANKL/RANK expression, which plays essential roles in osteoclastogenesis (21, 22, 56) and osteoclastic bone loss in RA as well as in AA (24). Treatment with PS liposomes significantly decreased the expression of RANKL and RANK in parallel with a significant reduction of trabecular bone loss in AA rats. It is considerable that there are at least three possible mechanisms underlying PS liposome-induced down-regulation of RANKL/RANK. First, PS liposomes decreased the expression levels of IL-1β and IL-17, which can promote the expression of RANKL (79, 80). Secondly, PS liposomes induced IL-10, which strongly inhibited the expression of RANKL/RANK (24, 70). Thirdly, as proved in chapter I, PS liposomes are phagocytosed by the osteoclast precursor to directly decrease the expression of RANK by osteoclast precursor and the production of RANKL in cultured rat bone marrow cells. Therefore, it is considered that the inhibitory effect of PS liposomes on the trabecular bone loss in AA rats completely depends on the inhibition of the RANKL/RANK pathway.

LPS, one of constituents of CFA, can activate MAPKs and NF-κB (81). The activity of MAPKs and NF-κB are involved in the regulation of cytokine production (82, 83, 84). According to our experimental design, a low concentration of LPS induced the activation of p38 MAPK, ERK and NF-κB in macrophages resulted in the release of IL-1β and IL-10. It was noted that PS liposomes rapidly reduced LPS-induced activation of p38 MAPK, but enhanced LPS-induced activation of ERK. This is the first study to examine the effects of PS liposomes on LPS-induced MAPK activation. These observations are consistent with previous observations that PS liposomes induce ERK but not p38 MAPK activity in primary cultured rat microglia (16) and macrophages (85). Therefore, it is reasonable to consider that lysosomal proteolytic functions are involved in LPS-induced MAPKs activity following phagocytosis of PS

liposomes. The inhibitory effects of PS liposomes on IL-1β secretion from LPS-activated macrophages may depend on the reduction of p38 MAPK activity, because p38 MAPK activity plays crucial roles in the regulation of IL-1β biosynthesis (86) and p38 MAPK inhibitor blocks IL-1β production (87). Furthermore, PSL-induced inhibition of NF-κB activity may be involved in the inhibition of IL-1β, because NF-κB activity is required for pro-inflammatory cytokine production, including IL-1β (84). However, PS liposome-induced increase in IL-10 by LPS-stimulated macrophages may depend on ERK activity, because ERK activity leads to IL-10 production (88, 89). Furthermore, PSL inhibited the rapid activation of p38 MAPK and may result in the subsequent slow enhancement of ERK activity in LPS-stimulated macrophages, because p38 MAPK and ERK cross-regulate each other such that the inhibition of one enhances the activation of the other (88, 90). Moreover, PS liposomes regulated the expression of IL-10 and IL-1β in the PB monocytes, the source of infiltrated macrophages in the ankle joints, and the activation of p-p38, p-ERK and p-IκBα in the infiltrated macrophages in synovial tissues of ankle joint of AA rats, thus indicated that systemic treatment with PS liposomes might effect on the monocytes/macrophages before and after infiltrated into synovium of ankle joints of AA rats. These observations strongly suggest that PS liposome-induced inhibition p38 MAPK and the subsequent enhancement of ERK is the most likely underlying mechanism for phenotypic change of infiltrated macrophages after phagocytosis of PS liposomes.

In conclusion, systemic treatment with PS liposomes inhibited AA-induced trabecular bone loss by provoking the phenotypic change of macrophages, from IL-1β-producing to IL-10-producing cells, in the ankle joint of AA rats. This phenotypic change of infiltrated macrophages is caused by the PS liposome-induced inhibition of p38 MAPK activity and the subsequent enhancement of ERK activity.

Conclusion

The current findings strongly suggest that phagocytosis of PS liposomes can strongly inhibit AA-induced bone loss through both the direct inhibitory effects on osteoclastogenesis and the indirect effects through changing the infiltrated macrophages from pro-inflammatory to anti-inflammatory phenotype.

Since PS is a competent of mammalian cell membranes, PS liposomes can be used as potential pharmacological interventions against inflammatory bone loss in RA and peritonitis without any apparent deleterious side effects

Acknowledgment

This work was carried out under supervision of professor Nakanishi, department of aging science and pharmacology, faculty of dental sciences, kyushu university. I would like to express sincere gratitude to his kind guidance, advice and support through this work. The author is grateful to Dr. Zhou Wu for guidance, technical advice and useful discussion. I also wish to thanks Dr. Hayashi for his kind help during my study in Japan. The contribution to this work by members and staffs of department of aging science and pharmacology, faculty of dental sciences, kyushu university, are greatly appreciated.

I would especially like to thank the Japanese Government, through Monbusho, for monetary support during this study.

Finally I would like to express my appreciation to my parents, my husband and my daughter, for their selfless understanding, supports and advice through all the four years' study.

References

1. Athanasou, N. A., and J. Quinn. Immunophenotypic differences between osteoclasts and macrophage polykaryons: immunohistological distinction and implications for osteoclast ontogeny and function. J. Clin. Pathol. 1990; 43: 997-1003.
2. Steinman, R. M., S. Turley, I. Mellman, et al. The induction of tolerance by dendritic cells that have captured apoptotic cells. J. Exp. Med. 2000; 191: 411-416.
3. Iyoda, T., S. Shimoyama, K. Liu, et al. The CD8+ dendritic cell subset selectively endocytoses dying cells in culture and in vivo. J. Exp Med. 2002; 195: 1289-302.
4. Boabaid, F., P. S. Cerri, and E. Katchburian. Apoptotic bone cells may be engulfed by osteoclasts during alveolar bone resorption in young rats. Tissue Cell 2001; 33: 318-325.
5. Cerri, P. S., F. Boabaid, and E. Katchburian. Combined TUNEL and TRAP methods suggest that apoptotic bone cells are inside vacuoles of alveolar bone osteoclasts in young rats. J. Periodontal. Res. 2003; 38: 223-226.
6. Schlegel, R. A., M. K. Callahan, and P. Williamson. The central role of phosphatidylserine in the phagocytosis of apoptotic thymocytes. Ann. NY Acad. Sci. 2000; 926: 217-225.
7. Zwaal, R. F., and A. J. Schroit. Pathophysiologic implications of membrane phospholipid asymmetry in blood cells. Blood. 1997; 89: 1121-1132.
8. Krahling, S., M. K. Callahan, P. Williamson, et al. Exposure of phosphatidylserine is a general feature in the phagocytosis of apoptotic lymphocytes by macrophages. Cell Death Differ. 1999; 6: 183-189.
9. Verhoven, B., S. Krahling, R. A. Schlegel, et al. Regulation of phosphatidylserine exposure and phagocytosis of apoptotic T lymphocytes.

Cell Death Differ. 1999; 6: 262-270.

10. Fadok, V.A., D.L. Bratton, D. M., Rose, et al. A receptor for phosphatidylserine-specific clearance of apoptotic cells. Nature. 2000; 405: 85-90.
11. Fadok, V. A., D. L. Bratton, A. Konowal, et al. Macrophages that have ingested apoptotic cells in vitro inhibit proinflammatory cytokine production through autocrine/paracrine mechanisms involving TGF-β, PGE2, and PAF. J. Clin. Invest. 1998;101: 890-898.
12. Hoffmann, P. R., A.M. deCathelineau, C. A. Ogden, et al. Phosphatidylserine (PS) induces PS receptor-mediated macropinocytosis and promotes clearance of apoptotic cells. J. Cell Biol. 2001; 155: 649-659.
13. Huynh, M. L., V. A. Fadok, and P. M. Henson. Phosphatidylserine-dependent ingestion of apoptotic cells promotes TGF-β1 secretion and the resolution of inflammation. J. Clin. Invest. 2002;109: 41-50.
14. Chen, X., K. Doffek, S. L. Sugg, et al. Phosphatidylserine regulates the maturation of human dendritic cells. J. Immunol. 2004;173: 2985-2994.
15. Otsuka, M., S. Tsuchiya, and Y. Aramaki. Invilvement of EK, A MAP kinase, in the production of TGF-β by macrophages treated with liposomes composed of phosphatidylserine. Biochem. Biophys. Res. Commun. 2004; 324: 1400-1405.
16. Zhang, J., S. Fujii, Z. Wu, et al. Involvement of COX-1 and up-regulated prostaglandin E synthases in phosphatidylserine liposome-induced prostaglandin E2 production by microglia. J. Neuroimmunol. 2006; 172: 112-120.
17. Shi, D., M. Fu, P. Fan, et al. Artificial phosphatidylserine liposome mimics apoptotic cells in inhibiting maturation and immunostimulatory function of murine myeloid dendritic cells in response to 1-chloro-2,4-dinitrobenze in vitro. Arch. Dermatol. Res. 2007; 299: 327-336.

18. Teitelbaum, S. L., and F.P. Ross. Genetic regulation of osteoclast development and function. Nat. Rev. Genet. 2003; 4: 638-649.
19. Miyamoto, T., O. Phneda, F. Arai, K. Iwamoto, et al. Bifurcation of osteoclasts and dendritic cells from common progenitors. Blood. 2001; 98: 2544-2554.
20. Kong Y.Y., H. Yoshida, I. Sarosi, et al. OPGL is a key regulator of osteoclastogenesis, lymphocyte development and lymph-node organogenesis. Nature. 1999; 397: 315-323.
21. Li, J., I. Sarosi, X. Q. Yan, et al. RANK is the intrinsic hematopoietic cell surface receptor that controls osteoclastogenesis and regulation of bone mass and calcium metabolism. Proc. Natl. Acad. Sci. 2000; 97: 1566-1571.
22. Dougall, W. C., M. Glaccum, K. Charrier, et al. RANK is essential for osteoclast and lymph node development. Genes Dev. 1999; 13: 2412-2424.
23. Kim, N., P. R. Odgren, D. K. Kim, et al. Diverse roles of the tumor necrosis factor family member TRANCE in skeletal physiology revealed by TRANCE deficiency and partial rescue by a lymphocyte-expressed TRANCE transgene. Proc. Natl. Acad. Sci. 2000; 97: 10905-10910.
24. Gravallese, E. M., C. Manning, A. Tsay, et al. Synovial tissue in rheumatoid arthritis is a source of osteoclast differentiation factor. Arthritis Rheum. 2000; 43: 250-258.
25. Tani-Ishii, N., J. M. Penninger, G. Matsumoto, et al. The role of LFA-1 in osteoclast development induced by co-cultures of mouse bone marrow cells and MC3T3-G2/PA6 cells. J. Periodont. Res. 2002; 37: 184-191.
26. Harada, H., T. Kukita, A. Kukita, et al. Involvement of lymphocyte function-associated antigen-1 and intercellular adhesion molecule-1 in osteoclastogenesis: a possible role in direct interaction between osteoclast precursors. Endocrinology 1998;139: 3967-3975.
27. Nakamura H, S. Kenmotsu, H. Sakai, et al. Localization of CD44, the

hyaluronate receptor, on the plasma membrane of osteocytes and osteoclasts in rat tibiae. Cell Tissue Res. 1995; 280: 225-233.

28. Kukita, A., T. Kukita, K. Hata, et al. Heat-treated osteoblastic cell (ROS17/2.8)-conditioned medium induces the formation of osteoclast-like cells. Bone Miner. 1993; 23: 113-127.
29. Kukita, A., T. Kukita, J. H. Shin, et al. Induction of mononuclear precursor cells with osteoclastic phenotypes in a rat bone marrow culture system depleted of stromal cells. Biochem. Biophys. Res. Commun. 1993; 196: 1383-1389.
30. Wu, Z., K. Nagata, and T. Iijima. Immunohistochemical study of NGF and its receptors in the synovial membrane of the ankle joint of adjuvant-induced arthritic rats. Histochem Cell Biol. 2000; 14: 453-459.
31. Wu, Z., K. Nagata, and T. Iijima. Involvement of sensory nerves and immune cells in osteophyte formation in the ankle joint of adjuvant arthritic rats. Histochem. Cell Biol. 2002; 118: 213-220.
32. Toh, K., T. Kukita, Z. Wu, et al. Possible involvement of MIP-1 in the recruitment of osteoclast progenitors to the distal tibia in rats with adjuvant-induced arthritis. Lab. Invest. 2004; 84: 1092-1102.
33. Damoiseaux, J.G., E. A Döpp, W. Calame, et al. Rat macrophage lysosomal membrane antigen recognized by monoclonal antibody ED1. Immunology 1994; 83: 140-147.
34. Shinar, D. M., and G. A. Rodan. Biphasic effects of transforming growth factor-on the production of osteoclast-like cells in mouse bone marrow cultures: the role of prostaglandins in the generation of these cells. Endocrinology 1990; 126: 3153-3158.
35. Yamaguchi, M., and S. Kishi. Differential effects of transforming growth factor osteoclast-like cell formation in mouse marrow culture: relation to the effect of zinc-chelating dipeptides. Peptides 1995; 16: 1483-1488.

36. Sato, T., I. Morita, K. Sakaguchi, et al. Involvement of prostaglandin endoperoxide H synthase-2 in osteoclast-like cell formation induced by interleukin-1 . J. Bone Miner Res.1996; 11: 392-400.

37. Hurley, M. M., S. K. Lee, L. G. Raisz, et al. Basic fibroblast growth factor induces osteoclast formation in murine bone marrow cultures. Bone 1998; 22: 309-316.

38. Okada, Y., A. Lorenzo, A. M. Freeman, et al. Prostaglandin G/H synthase-2 is required for maximal formation of osteoclast-like cells in culture. J. Clin. Invest. 2000; 105: 823-832.

39. Quinn, J. M., A. Sabokbar, M. Denne, M. C. de Vernejoul, et al. Inhibitory and stimulatory effects of prostaglandins on osteoclast differentiation. Calcif. Tissue Int. 1997; 60: 63-70.

40. Chenu, C., N. Kurihara, G. R. Mundy, et al. Prostaglandin E2 inhibits formation of osteoclast-like cells in long-term human marrow cultures but is not a mediator of the inhibitory effects of transforming growth factor. J. Bone Miner. Res. 1990; 5: 677–681.

41. Roux, S., F. Pichaud, J. Qinn, et al. Effects of prostaglandins on human hematopoietic osteoclast precursors. Endocrinology 1997; 138: 1476-1482.

42. Itonaga, I., A. Sabokbar, S. D. Neale, et al. 1, 25-Dihydroxyvitamin D3 and prostaglandin E2 act directly on circulating human osteoclast precursors. Biochem. Biophys. Res. Commun. 1999; 264: 590-595.

43. Wrana, J. L., L. Attisano, R. Wieser, et al. Mechanism of activation of the TGF-β receptor. Nature 1994; 370: 341-347.

44. Tanaka, M., A. Sakai, S. Uchida, et al. Prostaglandin E2 receptor (EP4) selective agonist (ONO-4819.CD) accelerates bone repair of femoral cortex after drill-hole injury associated with local upregulation of bone turnover in mature rats. Bone 2004; 34: 940-948.

45. Take, I., Y. Kobayashi, Y. Yamamoto, et al. Prostaglandin E2 strongly inhibits

human osteoclast formation. Endocrinology 2005; 146: 5204-5014.

46. Kaneki, H., I. Takagi, M. Fujieda, et al. Prostaglandin E2 stimulates the formation of mineralized bone nodules by a cAMP-independent mechanism in the culture of adult rat calvarial osteoblasts. J. Cell. Biochem. 1999; 73: 36-48.

47. Ramirez-Yañez, G. O., S. Hamlet, A. Jonarta, G. J. Seymour, and A. L. Symous. 2006. Prostaglandin E2 enhances transforming growth factor-β1 and TGF-β receptors synthesis: an in vivo and in vitro study. Prostaglandins Leukot Essent Fatty Acids. 74: 183-192.

48. Karsdal, M. A., P. Hjorth, K. Henriksen, et al. Transforming growth factor- controls human osteoclastogenesis through the p38 MAPK and regulation of RANK expression. J. Biol. Chem. 2003; 278: 44975-44987.

49. Karst, M., G. Gorny, R. J. Galvin, et al. Roles of stromal cell RANKL, OPG, and M-CSF expression in biphasic TGF-β regulation of osteoclast differentiation. J. Cell. Physiol. 2004; 200: 99-106.

50. Suda, T., N. Takahashi, and T. J. Martin. Role of vitamin D in bone resorption. J. Cell. Biochem. 1992; 49: 53-58.

51. Garcia-Palacios, V., H. Y. Chung, S. J. Choi, et al. Eosinophil chemotactic factor-L (ECF-L) enhances osteoclast formation by increasing in osteoclast precursors expression of LFA-1 and ICAM-1. Bone 2007; 40: 316-322.

52. Tomioka, H., T. Shimizu, W. W. Maw, et al. Roles of tumour necrosis factor-α (TNF-α), transforming growth factor-β (TGF-β1), and IL-10 in the modulation of intercellular adhesion molecule-1 (ICAM-1) expression by macrophages during mycobacterial infection. Clin. Exp. Immunol. 2000; 122: 335-342.

53. Takahashi H. K., H. Iwagaki, T. Yoshino, et al. Prostaglandin E2 inhibits IL-18-induced ICAM-1 and B7.2 expression through EP2/EP4 receptors in human peripheral blood mononuclear cells. J. Immunol. 2002; 168: 4446-

4454.

54. Sela, U., N. Mauermann, R. Hershkoviz, et al. The inhibition of autoreactive T cell functions by a peptide based on the CDR1 of an anti-DNA autoantibody is via TGF-β-mediated suppression of LFA-1 and CD44 expression and function. J. Immunol. 2005; 175: 7255-7263.

55. Asagiri, M., T. Hirai, T. Kunigami, et al. Cathepsin K-dependent toll-like receptor 9 signaling revealed in experimental arthritis. Science 2008; 319: 624-627.

56. Kong Y. Y., U. Feige, I. Sarosi, et al. Activated T cells regulate bone loss and joint destruction in adjuvant arthritis through osteoprotegerin ligand. Nature 1999; 402: 304-309.

57. Marcelli, C., A. J. Yates, and G. R. Mundy. In vivo effects of human recombinant transforming growth factor beta on bone turnover in normal mice. J. Bone Miner. Res. 1990; 5: 1087-1096.

58. Yoshida, K., H. Oida, T. Kobayashi, et al. Stimulation of bone formation and prevention of bone loss by prostaglandin E EP4 receptor activation. Proc. Natl. Acad. Sci. 2002; 99: 4580-4585.

59. Serhan CN, Savill J. Resolution of inflammation: the beginning programs the end. Nat Immunol 2005; 6:1191-1197.

60. Serhan CN, Brain SD, Buckley CD, et al. Resolution of inflammation: state of the art, definitions and terms. FASEB J 2007;21:325-232.

61. Byrne A, Reen DJ. Lipopolysaccharide induces rapid production of IL-10 by monocytes in the presence of apoptotic neutrophils. J Immunol 2002;168: 1968-1977.

62. Steinman RM, Turley S, Mellman I, et al. The induction of tolerance by dendritic cells that have captured apoptotic cells. J Exp Med 2000;191:411-416.

63. Hoffmann PR, Kench JA, Vondracek A, et al. Interaction between

phosphatidylserine and the phosphatidylserine receptor inhibits immune responses in vivo. J Immunol 2005;174:1393-1404.

64. Ramos GC, Fernandes D, Charão CT, et al. Apoptotic mimicry: phosphatidylserine liposomes reduce inflammation through activation of peroxisome proliferator-activated receptors (PPARs) in vivo. Br J Pharmacol 2007;151:844-50.

65. Wu Z, Ma HM, Kukita T, et al. Phosphatidylserine-containing liposomes inhibit the differentiation of osteoclasts and trabecular bone loss. J Immnunol 2010; 184: 3191-3201.

66. Ji H, Pettit A, Ohmura K, et al. Critical roles for interleukin 1 and tumor necrosis factor-α in antibody-induced arthritis. J Ex Med 2002;196:77-85.

67. Karouzakis E, Neidhart M, Gay RE, et al. Molecular and cellular basis of rheumatoid joint destruction. Immunol Lett 2006;106:8-13.

68. Kotake S, Udagawa N, Takahashi N, et al. IL-17 in synovial fluids from patients with rheumatoid arthritis is a potent stimulator of osteoclastogenesis. J Clin Invest. 1999;103:1345-1352.

69. Chabaud M and Miossec P. The combination of tumor necrosis factor alpha blockade with interleukin-1 and interleukin-17 blockade is more effective for controlling synovial inflammation and bone resorption in an ex vivo model. Arthritis Rheum 2001; 44:1293-1303.

70. Van de Loo FA, van den Berg WB. Gene therapy for rheumatoid arthritis. Lessons from animal models, including studies on interleukin-4, interleukin-10, and interleukin-1 receptor antagonist as potential disease modulators. Rheum Dis Clin North Am 2002; 28:127-149.

71. Zhang X, Teng YT. Interleukin-10 inhibits gram-negative-microbe-specific human receptor activator of NF-κB ligand-positive $CD4^+$ Th1-cell-associated alveolar bone loss in vivo. Infect Immun 2006; 74:4927-4931.

72. Terrier F, Hricak H, Revel D, et al. Magnetic resonance imaging and spectroscopy of the periarticular Inflammatory soft-tissue changes in experimental arthritis of the rat. Invest Radiol 1985; 20:813-823.
73. Wu Z, Zhang J, Nakanishi H. Leptomeningeal cells activate microglia and astrocytes to induce IL-10 production by releasing pro-inflammatory cytokines during systemic inflammation. J Neuroimmunol 2005; 167:90-98.
74. Klareskog L, Ronnelid J, Holm G. Immunopathogenesis and immunotherapy in rheumatoid arthritis: an area in transition. J Inter Med 1995;238: 191-206.
75. Muller-Ladner U, Pap T, Gay RE, et al. Mechanisms of disease: the molecular and cellular basis of joint destruction in rheumatoid arthritis. Nat Clin Pract Rheumatol 2005;1:102–110.
76. Asagiri M, Hirai T, Kunigami T, et al. Cathepsin K-dependent toll-like receptor 9 signaling revealed in experimental arthritis. Science 2008; 319:624-627.
77. Acosta-Rodriguez EV, Napolitani G, Lanzavecchia A et al. Interleukins 1β and 6 but not transforming growth factor-β are essential for the differentiation of interleukin 17-producing human T helper cells, Nat Immunol. 2007; 8: 942–949.
78. Chang H, Hanawa H, Yoshida T, et al. Alteration of IL-17 related protein expressions in experimental autoimmune myocarditis and inhibition of IL-17 by IL-10-Ig fusion gene transfer. Circ J. 2008; 72: 813-819.
79. Suda T, Takahashi N, Udagawa N, et al. Modulation of osteoclast differentiation and function by the new member of the tumor necrosis factor receptor and ligan families. Endocrine Reviews 1999; 20: 345-357.
80. Ju JH, Cho ML, Moon YM, et al. IL-23 induces receptor activator of NF-κB ligand expression on $CD4^+$ T cells and promotes osteoclastogenesis in an autoimmune arthritis model. J Immunol 2008;181:1507-1518.
81. Sweet MJ, Hume DA. Endotoxin signal transduction in macrophages. J Leukoc Biol 1996; 60:8-26.

82. Lee JC, Laydon JT, McDonnell PC, et al. A protein kinase involved in the regulation of inflammatory cytokine biosynthesis. Nature 1994; 372:739–746.

83. Feng GJ, Goodridge HS, Harnett MM, et al. Extracellular signal-related kinase (ERK) and p38 mitogen-activated protein (MAP) kinases differentially regulate the lipopolysaccharide-mediated induction of inducible nitric oxide synthase and IL-12 in macrophages: Leishmania phosphoglycans subvert macrophage IL-12 production by targeting ERK MAP kinase. J Immunol. 1999; 163:6403–6412.

84. Simmonds RE, Foxwell BM. Signalling, inflammation and arthritis: NF-κB and its relevance to arthritis and inflammation. Rheumatology 2008; 47:584-590.

85. Aramaki Y, Matsuno R, Tsuchiya S. Involvement of p38 MAP kinase in the inhibitory effects of phosphatidylserine liposomes on nitric oxide production from macrophages stimulated with LPS. Biochem Biophys Res Commun. 2001; 280: 982-987.

86. Baldassare JJ, Bi Y, Bellone CJ. The role of p38 mitogen-activated protein kinase in IL-1β transcription. J Immunol 1999;162:5367–53.

87. Lee SJ, Lim KT. Phytoglycoprotein inhibits interleukin-1β and interleukin-6 via p38 mitogen-activated protein kinase in lipopolysaccharide-stimulated RAW 264.7 cells. Naunyn Schmiedebergs Arch Pharmacol 2008;377:45-54.

88. Mathur RK, Awasthi A, Wadhone P, et al. Reciprocal CD40 signals through p38 MAPK and ERK-1/2 induce counteracting immune responses. Nat Med. 2004;10:540-544.

89. Lucas M, Zhang X, Prasanna V, et al. ERK activation following macrophage FcγR ligation leads to chromatin modifications at the IL-10 locus. J Immunol 2005; 175:469-477.

90. Kim C, Sano Y, Todorova K, et al. The kinase p38α serves cell type-specific

inflammatory functions in skin injury and coordinates pro- and anti-inflammatory gene expression. Nat Immunol 2008; 9:1019-1027.